Bismuth Based Thermoelectric Materials for Cooling

Undergraduate Honors Thesis

Presented in Partial Fulfillment of the Requirements for

Graduation with Distinction

at The Ohio State University

By

Katherine Whitehouse

* * * * *

The Ohio State University

2010

Defense Committee:

Professor Joseph Heremans, Advisor

Professor Yann Guzennec

ABSTRACT

Thermoelectric (TE) devices are solid state heat engines currently used in small coolers, air conditioning systems, and devices that generate electrical energy from heat, such as the exhaust of automobiles. These devices directly convert electricity to thermal energy or vice-versa. They have no moving parts, create no noise or vibrations, require no maintenance, are extremely reliable, and can be used at any scale. The major disadvantage is that these devices are less efficient than traditional cooling or power conversion methods. Recent research at the Ohio State University (OSU) resulted in a doubling of the efficiency of TE devices by the use of a new physical principle, resonant impurities, in lead telluride (Heremans, Javovic and Toberer). More recent research funded by the Japanese auto industry focuses on the development of thermoelectric materials that do not contain rare or toxic elements, such as lead and tellurium. This undergraduate research project focuses on improving the efficiency of bismuth-antimony alloys for cooling applications, by identifying resonant impurities in polycrystalline elemental bismuth, then bismuth-antimony alloys. Very little is known about the electrical effects of impurities other than tin, lead and tellurium in bismuth. During the course of the project, trace amounts of several elements were alloyed into bismuth with varying results. Preliminary experiments seem to indicate that indium might significantly improve the thermoelectric efficiency of bismuth, thus possibly opening a new class of thermoelectric alloys suitable for thermoelectric cooling applications.

ACKNOWLEDGMENTS

.

I would like thank everyone that helped me during this project. I am grateful for the guidance of Professor Heremans throughout this project. I would also like to thank all of the students in the Thermal Materials Lab, especially Chris Jaworski and Hyungyu Jin for all of the help they have given me.

TABLE OF CONTENTS

Page

LIST OF FIGURES

CHAPTER 1
INTRODUCTION

1.1 Introduction

Recent years have seen an increase in public interest and research into sources of renewable energy. Over half of the energy generated in the U.S. is lost due to inefficiencies, mainly into heat (Figure 1). Industry and researchers are looking for ways to improve efficiency, and thermoelectric technology is a way to do this. Thermoelectric materials have two distinct usages, power generation and heating or cooling applications. In this work, the focus was only on thermoelectric materials for cooling.

Thermoelectric materials traditionally have low efficiencies, but current low temperature materials (below 300K) have poor efficiencies even compared to other thermoelectric materials. The currently the leading materials for cooling at room temperature include tellurium, an extremely rare element. For cryogenic cooling, bismuth-antimony alloys are the current leader.

This research had two main parts. The majority of this project focuses on polycrystalline bismuth doped with small amounts of other elements and a smaller part of the research investigates nano-particle bismuth-antimony alloys with nano-inclusion of alumina. The purpose being to investigate the possibilities of a bismuth-based material that would not include rare materials or toxic materials while simultaneously improving overall efficiency.

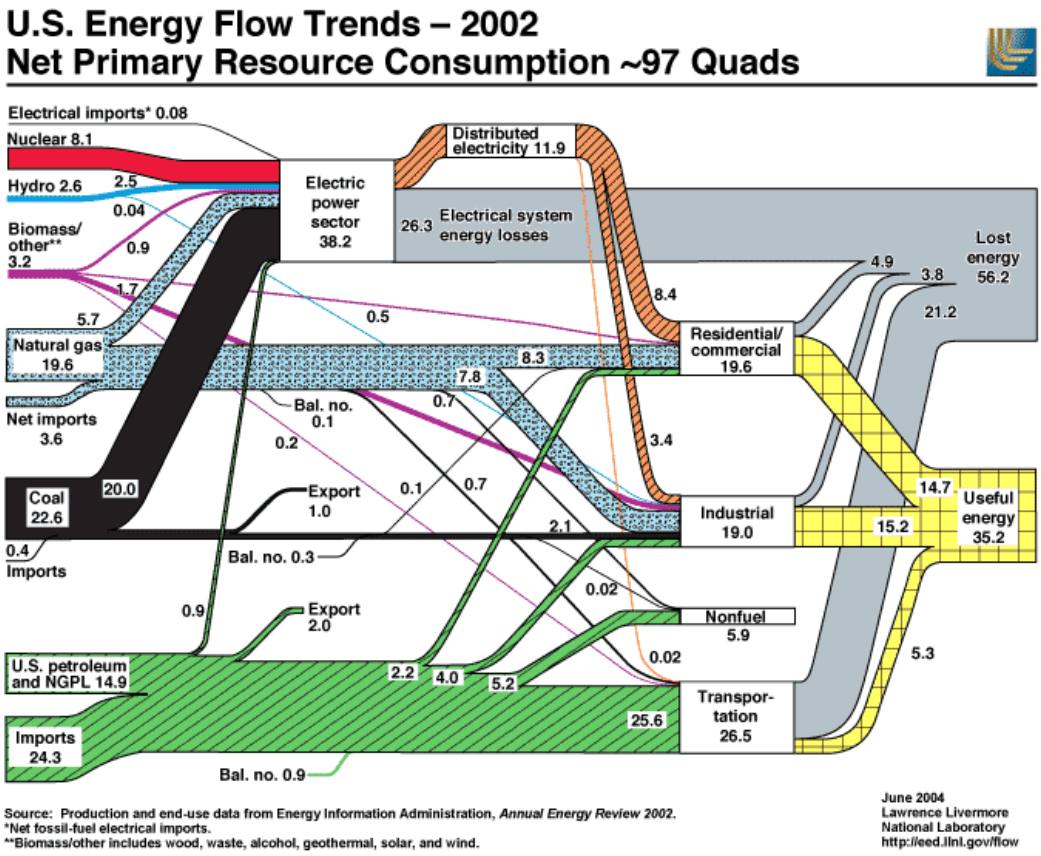

Figure 1: US Energy Consumption

1.3 Motivation

The need for portable and reliable cryogenic cooling is the driving force behind the main part of this project. Thermoelectric devices have many benefits. These devices have no moving parts and will never wear out, make noise or vibrate. The devices require no maintenance and are very reliable. They can also be scaled to any size. The major drawback to these devices is their efficiency. While efficiencies have improved greatly in recent years, these devices can still not compete with traditional heating and cooling

methods. They are primarily suited for niche applications where their reliability and power density outweigh their inefficiency.

Applications for these materials include refrigeration, cryogenic cooling and climate control. By replacing the current AC compression cycle in an automobile, these materials may have the ability to lower the energy used to cool a car as well as make the process faster. These materials are currently on the market, being used in camping equipment, cpu coolers, and small, specialized refrigerators.

The Department of Defense Research and Engineering (DDRE), the Air Force Office of Scientific Research (AFORSR), and the Multi University Research Initiative (MURI) are interested in cryogenic cooling for several applications and have recently awarded a 7.5 million dollar grant to fund this project and others like it.

The performance of integrated circuit (IC) dies, seen in

Figure 2, are limited by temperature. As they heat up during use, performance is reduced. Thermoelectric devices are able to cool the dies, reaching temperatures near 100K, while taking up very little space and significantly improving the die's computational speed (Stein).

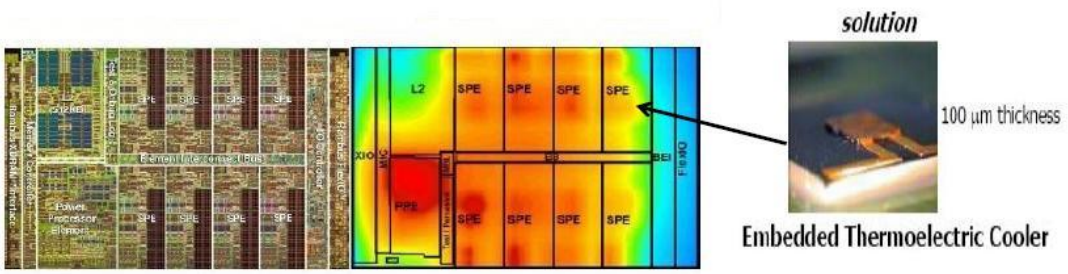

Figure 2: IC Die Heat Map(Stein)

Thermoelectric coolers can significantly extend the life of Reliability-Aware Microprocessors (RAMP), which are used on deep space probes. The RAMPs therefore need to be small and are required to last the lifetime of the probe, however, as the devices get smaller, their life expectancy is reduced, as seen in

Figure 3.

This effect can be negated keeping the RAMPS very cool through the use of thermoelectric coolers.

Figure 4 shows the relationship between mean time to failure and temperature (Stein)

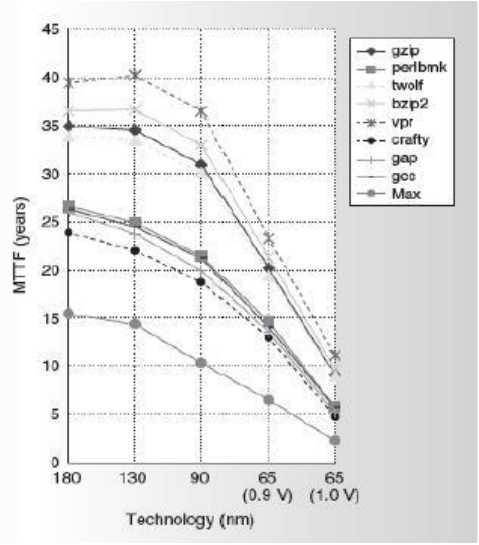

.

Figure 3: Mean Time to Failure vs. Size(Stein)

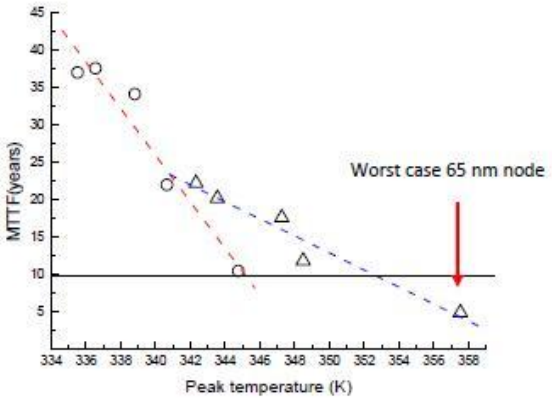

Figure 4: Mean time to Failure vs. Temperature(Stein)

Solid state coolers could also benefit defense satellites and reconnaissance drones. These devices include Space Situational Awareness Systems (SSA), Space Tracking and Situational System (STSS) a missile tracking and target discrimination system, Space Based Infrared System (SBIRS) an infrared missile warning system and an alternative space based infrared system (AIRSS). These system that work with all types of infrared wavelengths and many of the sensors on these devices must be cooled to 10K (Table 1). Cold body target discrimination is the driving force behind the low temperature requirement. Figure 5 shows the current devices produced by Lockheed Martin and Northrop Grumman used for that purpose. These devices weigh about 200kg per Watt of cooling capacity produced and are very inefficient, producing one watt of cooling for every 900 watts used(Stein). While thermoelectric devices would likely have a similar efficiency, they do have a high power density and therefore have the potential to produce the same power and weigh less than current technology. Weight is a significant factor for satellites and unmanned reconnaissance drones because of the power required to get them into space or fly them.

Table 1: Systems and Cooling Requirements(Stein)

System	System Wavelength Range	Required Temp
Space Situational Awareness System	X-Ray Y-Ray	<=10K
Missile Warning Space Electronics	Short/Medium Wavelength Infrared	<150K ~100K
Space Tracking Situational System Space Based Infrared Systems Intelligence, surveillance and reconnaissance aircraft	Long Wavelength Infrared	35/85K
Space Tracking Situational System Hyper-Spectral Imaging	Very Long Wavelength Infrared	10K

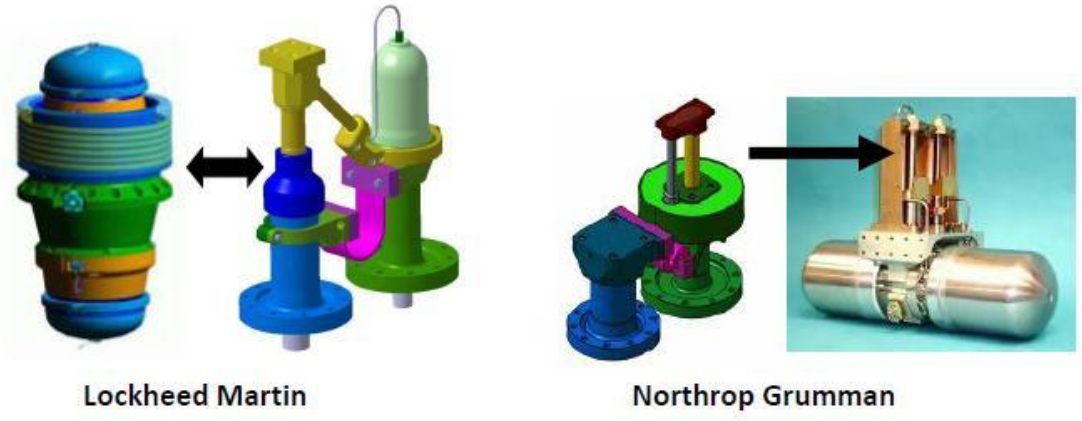

Figure 5: Current Cooling Technology(Stein)

1.4 Project Objective

The goal of this research is to develop the foundation for a high efficiency bismuth-antimony thermoelectric material for cooling by finding resonant impurities that are able to improve the thermoelectric properties of polycrystalline bismuth. The figure of merit (zT) is a non-dimensional term that relates to efficiency. Bismuth-antimony alloys currently have the highest figure of merit under 200K. However, zT is still quite low compared to best high temperature materials as seen in Figure 6. One reason in the factor T in zT. Very little is known about the effects of dopants in bismuth-antimony besides zinc, lead and tellurium. Polycrystalline bismuth-antimony can be a challenge to produce, so in the interest of time and simplicity, this project focuses on polycrystalline bismuth. The effects of impurities in polycrystalline bismuth are likely to translate into bismuth-antimony alloys. This is because bismuth-antimony alloys are typically bismuth rich, usually 88at% bismuth. Even with the substitution of antimony in the bismuth

crystals, the crystal symmetry is maintained, thus maintaining most of its electronic properties.

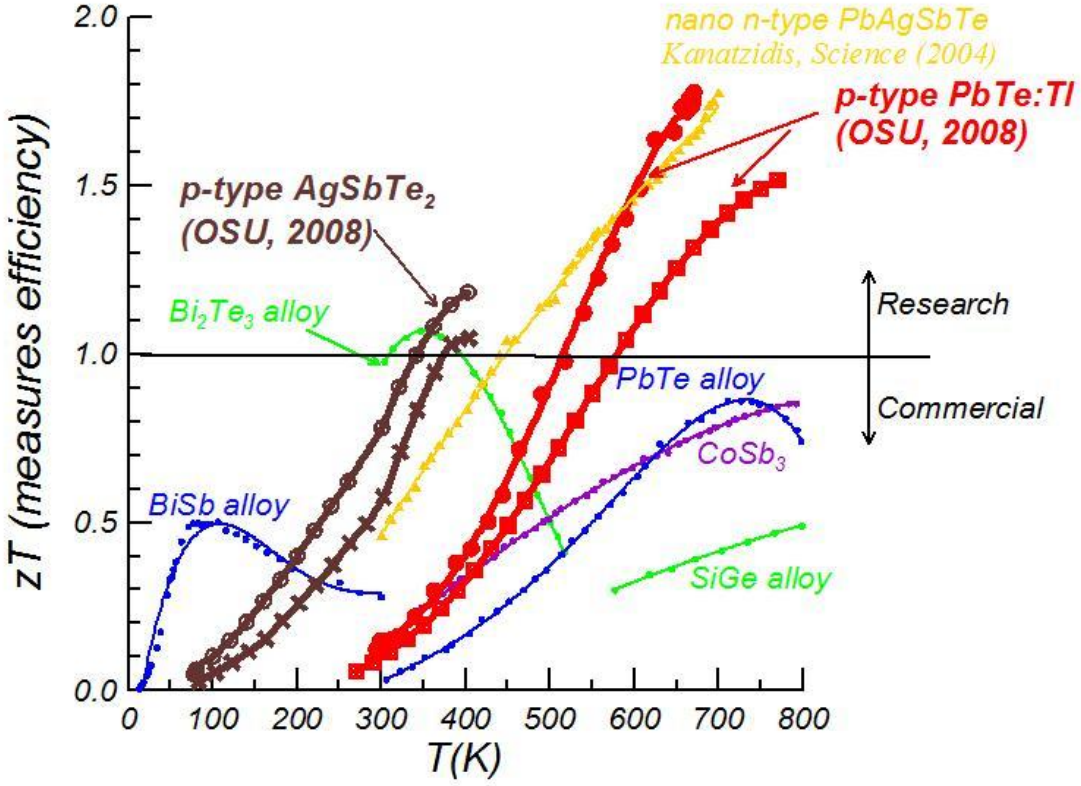

Figure 6: Current Thermoelectric Material Efficiencies(Jaworski)

CHAPTER 2
BACKGROUND

The principles behind thermoelectric devices have been around since the 1820's and 1830's with the discoveries of Seebeck and Peltier. It is the Seebeck effect that allows the measurement of temperature with thermocouples. Not until the mid twentieth century did thermoelectric devices become somewhat practical with breakthroughs made by Maria Telkes in semiconductor technology, creating the first thermoelectric generator and refrigerator(Dawson). Since then great strides have been made in improving the efficiency of these devices, particularly in the past 15 years (Figure 7).

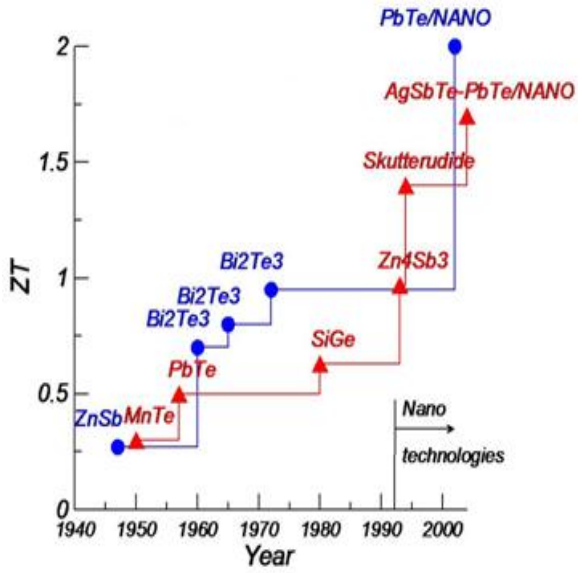

Figure 7: History of Thermoelectric Materials(Jaworski)

Thermoelectric devices are based on the Peltier effect. The Peltier effect refers to the release or absorption of heat from the junction of two dissimilar materials when a current is applied across it, depending on the direction of the current and the metals used.

This effect is best seen if the pairs of metals are opposite types. There are two types of thermoelectric materials, p-type and n-type. Thermoelectric devices use pairs of p-type and n type materials. The pairs are arranged in parallel and connected in series such that all n-to-p type connections are on one side of the device and all p-to-n type connections are on the other side as seen in Figure 8. When a current is run through the pairs, one side will release energy, while the other absorbs energy. Thus, one side of the device will get hot, and the other will get cold. A specific temperature difference will develop across the device for a given voltage applied. The hot and cold sides of the device can be switched by simply reversing the direction of current.

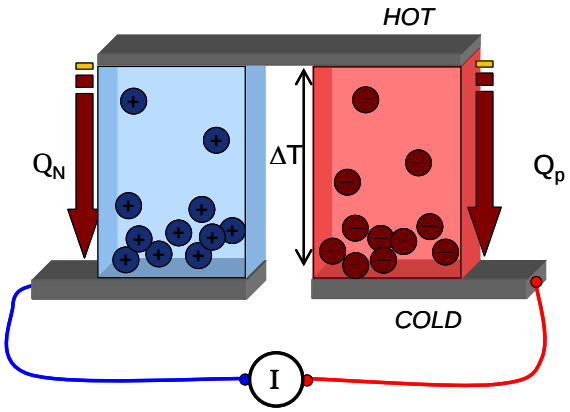

Figure 8: Heat Pump (Jaworski)

The Seebeck coefficient or thermoelectric power refers to a material's ability to directly convert thermal energy into electrical energy. The Seebeck effect is the principle behind thermocouples. When the junction of two metals are exposed to a temperature while the other ends are held at a reference temperature, a voltage will develop, given by the following equation:

$$V = (S_B - S_A)(T - T_{ref})$$

Where S_A and S_B are the Seebeck coefficient for the two materials. P-type and N-type semiconductors have opposite signs on their Seebeck coefficients, making them ideal pairs because they will add to make the resulting voltage larger. From this equation, it is also clear why a large magnitude Seebeck coefficient is desirable, the larger the Seebeck the larger the resulting voltage with a given temperature difference. This effect is used for power generation.

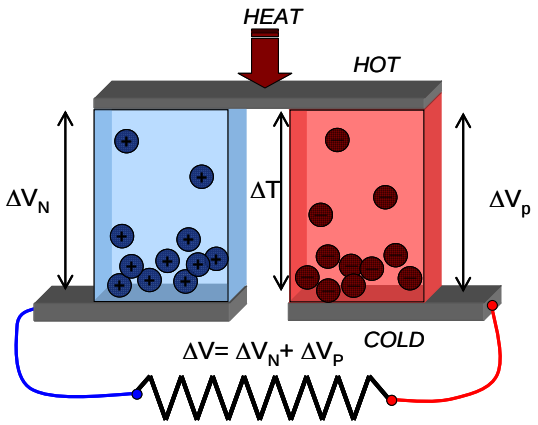

Figure 9: Power Generator (Jaworski)

The efficiency of thermoelectric materials is related to the figure of merit (zT) which is calculated using the following equation:

$$zT \equiv \frac{S^2 \sigma}{\kappa} T$$

Where S is the Seebeck coefficient in V/K, σ is electrical conductivity in Ω^{-1}-m^{-1}, κ is thermal conductivity in W/m-K and T is the temperature in Kelvin. From this equation, it can be seen that a high efficiency thermoelectric material would have a high Seebeck, a high electrical conductivity and a low thermal conductivity. These properties are

interrelated, increasing a material's Seebeck coefficient typically lowers its electrical conductivity, or raising the electrical conductivity also increased thermal conductivity For a power generator, zT relates to efficiency according to the following equation:

$$\eta = \frac{\Delta T}{T_{Hot}} \cdot \frac{\sqrt{1+zT}-1}{\sqrt{1+zT}+\frac{T_{Cold}}{T_{Hot}}}$$

For a heat pump, zT relates to the coefficient of performance.

CHAPTER 3
EXPERIMENTAL PROCEEDURE

Two main stages were involved in performing this research; sample synthesis and characterization. The goal was to make polycrystalline bismuth doped with small amounts of various elements, usually to the solubility limits. First, roughly seven grams of bismuth was measured and placed in a quartz ampoule, 10mm in diameter. From the exact amount of bismuth added, the required amount of the doping element was calculated. The doping element was then weighed out to an accuracy of +/- 0.00005g and added to the quartz ampoule. If the doping element was prone to oxidation, this process would be performed in a glove box filled with argon gas and an O_2 level of less than 0.1 ppm. When this was complete, I would evacuate the ampoule using a standard mechanical pump in combination with an oil diffusion pump, ultimately reaching 10^{-6} torr. This process takes roughly 12 hours.

After all the gasses had been removed, the ampoule was sealed using a propane torch. Upon heating the quartz locally, it collapses on itself do to the vacuum in the ampoule, this forming an airtight seal. The sample was heated above the melting point of both elements, unless the doping element has a melting point above 1200°C. The sample could not be heated above 1200°C because that is the highest temperature the ovens could reach. Then the sample was removed from the oven and immediately quenched in water.

If the sample was allowed to cool without quenching for more than a few seconds, single crystals would begin to form.

Once the sample was created, it needed to be tested. First, I tested the sample to be sure it is polycrystalline. If it is polycrystalline, the properties should be isotropic, if it is single crystal, the properties would be anisotropic due to the anisotropic rhombohedral crystal structure of bismuth. To test isotropy, I tested Seebeck in the three coordinate directions. To do this, the sample was placed on a heated copper pad while the temperature was measured on both sides simultaneously using a differential thermocouple. Then the voltage difference was divided by the temperature difference. If the results for all three directions were the same, the sample was polycrystalline.

I utilized two separate apparatuses with differing capabilities to characterize the samples in this thesis. One is a homebuilt cryostat; the other is the Thermal Transport Option (TTO) in the Quantum Design Physical Properties Measurement System (PPMS). The cryostat is cooled with liquid nitrogen and has a temperature range of 77K to 420 K where as the PPMS is cooled with liquid helium, allowing measurement to 2K. The cryostat is placed in an H-frame copper solenoid electro magnet which reaches a maximum of ±1.5 Tesla, where as the PPMS has a superconducting magnet, and can reach ±7 Tesla. The cryostat is configured to take equilibrium measurements at fixed temperatures while the TTO continuously takes measurements while sweeping temperature at a constant rate. However, the cryostat can perform a full sample characterization at one time, whereas the ppms would need to run twice to get all the measurements the cryostat makes. Both setups require the sample to be cut into a

rectangular prism roughly 2mm by 2mm by 8mm. For the PPMS, three copper wires are attached to the sample using silver epoxy, two along the length of the sample and on top. The sample is then attached to a copper base and connected to a sample puck which is placed in the liquid helium tank for testing. A computer program runs the desired test, and reports the results.

For the cryostat, two copper wires were spot welded about 6mm apart on one of the rectangular faces of the sample. This is accomplished using a capacitor attached to two pairs of tweezers. The sample was held in one and the wire was held by the other. When the wire touches the sample, a spot weld was formed. On the opposite face two t-type thermocouples, copper-constantan, were attached at the same distance apart as the copper wires on the opposite side. The constantan wires were attached using a silver epoxy. Then a copper wire was attached to the square top. The sample was then attached to a alumina pad with small copper plate on the bottom and top, again using silver epoxy. A small strain gage, used as a heater, was attached to the top of the sample above the copper plate. Thicker, coated copper wires were soldered to the alumina base. The wires from the sample are wound around the exposed ends of the soldered wires. The sample is then placed in the cryostat for testing. First, the coated copper wires are soldered to pins on the cryostat. These pins connect to wires that run down the length of the cryostat and attach to plugs at the other end. One copper shield and two aluminum shields are used to insulate the sample from outside heat or interference. Once the shields are attached, the tip of the cryostat, containing the sample, is placed in an electromagnet, used to create the magnetic field required for testing. The plugs on the cryostat were connected to the

instrumentation. Several checks were then performed to ensure all the connections were working properly. A model of the prepared sample can be seen in Figure 10.

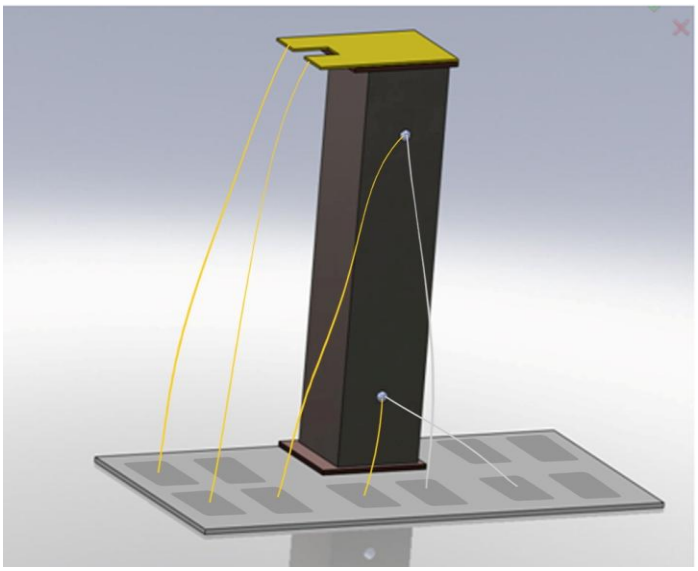

Figure 10: Prepared Cryostat Sample

Once in the cryostat, a LabVIEW program is used to execute the testing. The sample is tested at temperatures ranging from 80K to 420K in increments of 20K. At each increment, the sample is subjected to a range of magnetic fields and data is recorded for each of the wires attached to the sample and saved into text files. After the LabVIEW program is complete, the text files are read into a MathCad program to process the data. From the MathCad program, data about the samples properties can be obtained.

Because of the extremely low solubility levels of many of the dopants and the very small amounts added to the samples, in some cases, it was prudent to check the composition of the samples. One method for checking the composition was to analyse

the samples magnetic properties. Each element has a different magnetic signature, thus by looking at the samples magnetic signature, the composition could be obtained.

If more accurate data was required, as in the case of the indium sample, Ohio State's Research Reactor was used to perform Neutron activation analysis. Each element decays differently. Bismuth has very little reaction whereas Indium has a significant reaction. First, a sample of pure indium was tested at a specific power level for a specific amount of time. The results were used as a benchmark to measure the indium levels in other samples. The bismuth-indium sample was tested at the same power level and length of time. From the results, the mass of indium in the sample can be calculated based on the pure indium sample. With that, the weight percentage and thus the atomic percentage was calculated.

CHAPTER 4
POLYCRYSTALLINE BISMUTH WITH DOPANTS

4.1 Introduction

Various elements were selected to test as dopants for polycrystalline bismuth. Samples compositions were based on the solubility limits of the dopants in bismuth when that information was available. For several elements, the solubility was unknown so an arbitrary value was selected to test. Table 2 shows the solubility limits of a selection of elements in bismuth. The elements tested include gold, iridium, osmium, boron, indium, gallium and aluminum.

Table 2: Solubility Limits in Bismuth (Hansen)

Dopant	Solubility in Bi (at%)	Dopant2	Solubility in Bi (at%)3	Dopant4	Solubility in Bi (at%)5
Ag	0	H	0	Pr	Unknown
Al	1	Hg	Unknown	Pt	1.2
As	0.2	In	0.5	Pu	0.6
Au	Unknown	Ir	0.3	Rb	Unknown
B	0	K	Unknown	Rh	1.4
Ba	Unknown	La	Unknown	Ru	Unknown
Be	0	Li	Unknown	S	Unknown
C	0	Mg	Unknown	Sb	100
Ca	Unknown	Mn	1.9-3	Se	1
Cd	3	Mo	Unknown	Si	Less than 1.5%
Ce	Unknown	N	0	Sn	1.7 to 4.1
Co	0.032-0.035	Na	3.86	Sr	Unknown

Cr	Unknown	Ni	Unknown	Te	1.6 to 2.4
Cs	Unknown	Os	0.0044	Th	Unknown
Cu	Less than 3E-4	P	0.7	Ti	Unknown
Fe	Less than 7.5E-4	Pb	0.5 to 1	Tl	Less than 0.5
Ga	0.5	Pd	2.25	U	Unknown
Ge	1.5	Po	5E-10	Zn	6.1 to 11.8

4.2 Gold

One of the first samples to be tested was bismuth doped with gold. The composition chosen was $Bi_{99.7}Au_{0.3}$ because the solubility of gold in bismuth is unknown. This sample did not yield positive results. Figure 11 shows that gold had virtually no effect on thermal conductivity. Changes in thermal conductivity were not expected based on the small amounts of dopant material. Electrical resistivity slightly decreased, Figure 12. The biggest impact gold had on the bismuth can be seen in **Error! Reference source not found.**. Gold significantly reduced the Seebeck, resulting in a significantly reduced figure of merit as seen in Figure 14. We conclude that gold is an n-type dopant in bismuth. This is in contrast to silver, which has a slight p-type effect.

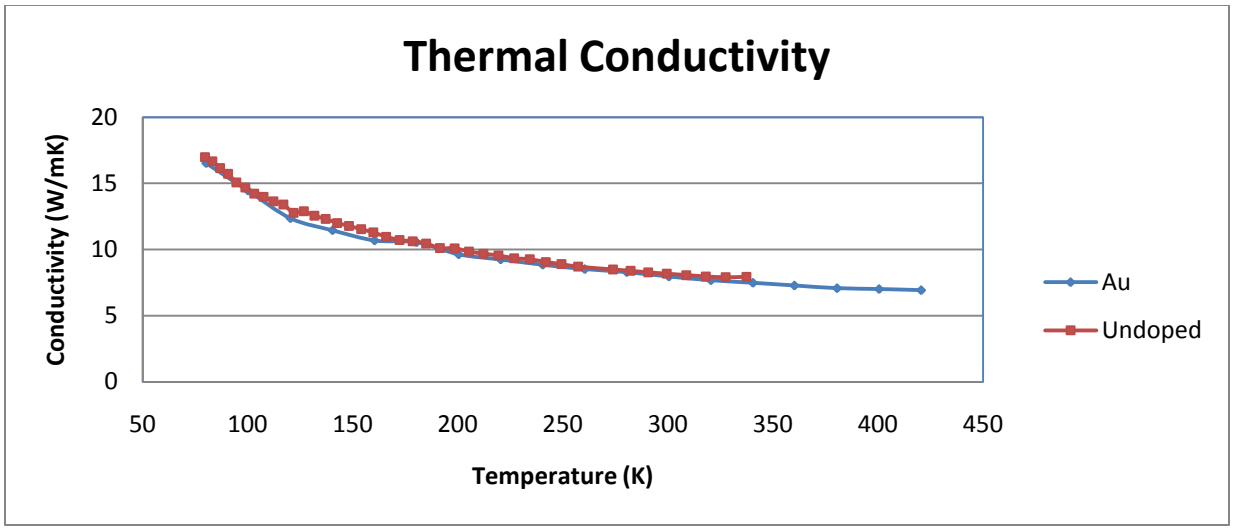

Figure 11: Thermal Conductivity of Gold Doped Bismuth

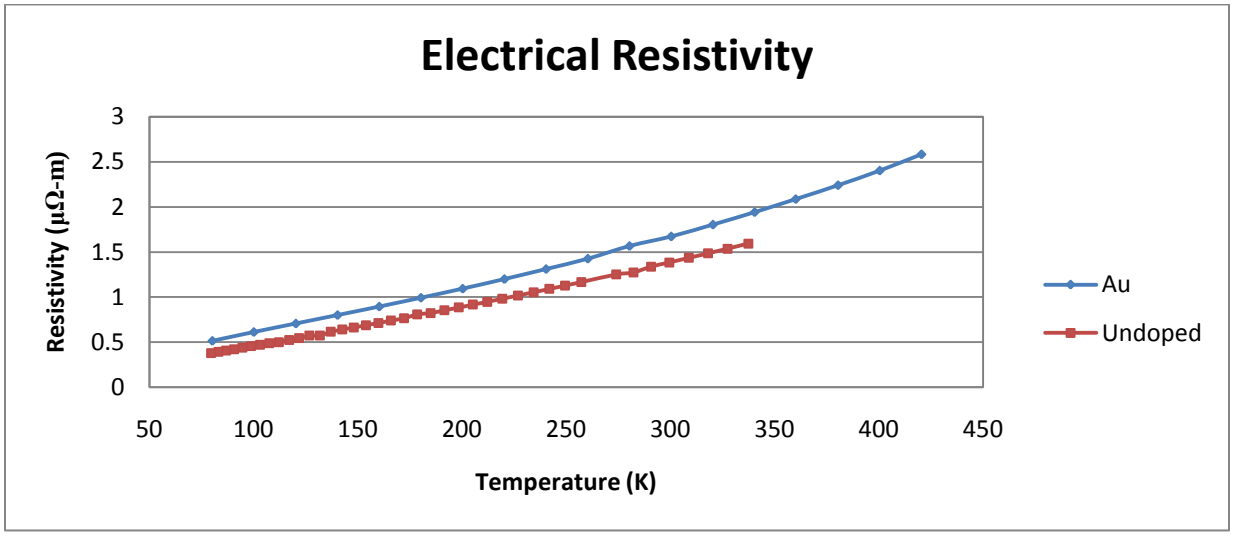

Figure 12:Electrical Resistivity of Gold Doped Bismuth

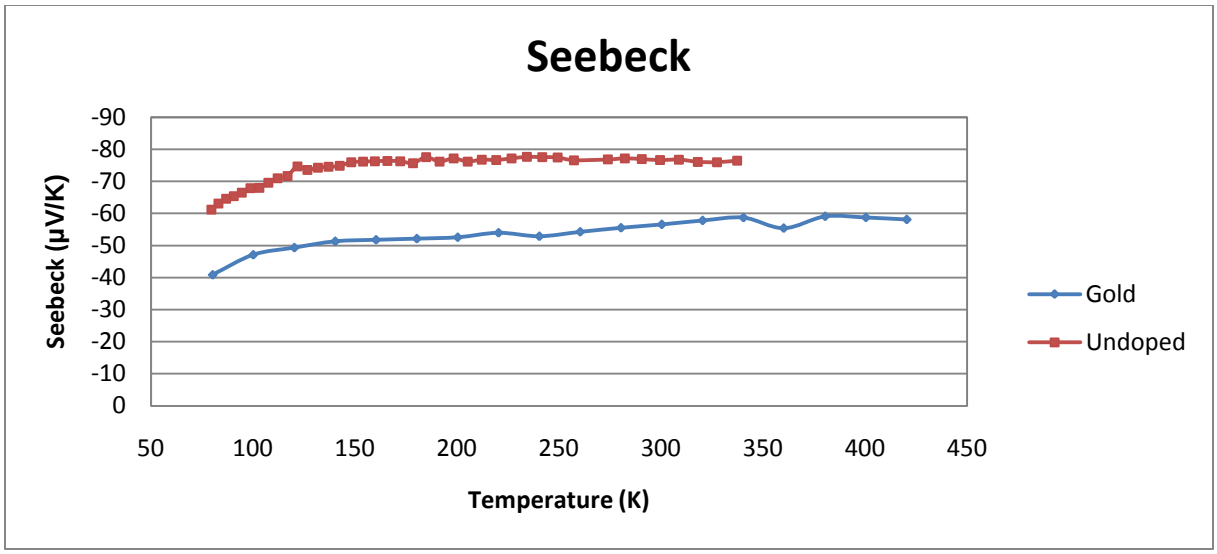

Figure 13:Seebeck of Gold Doped Bismuth

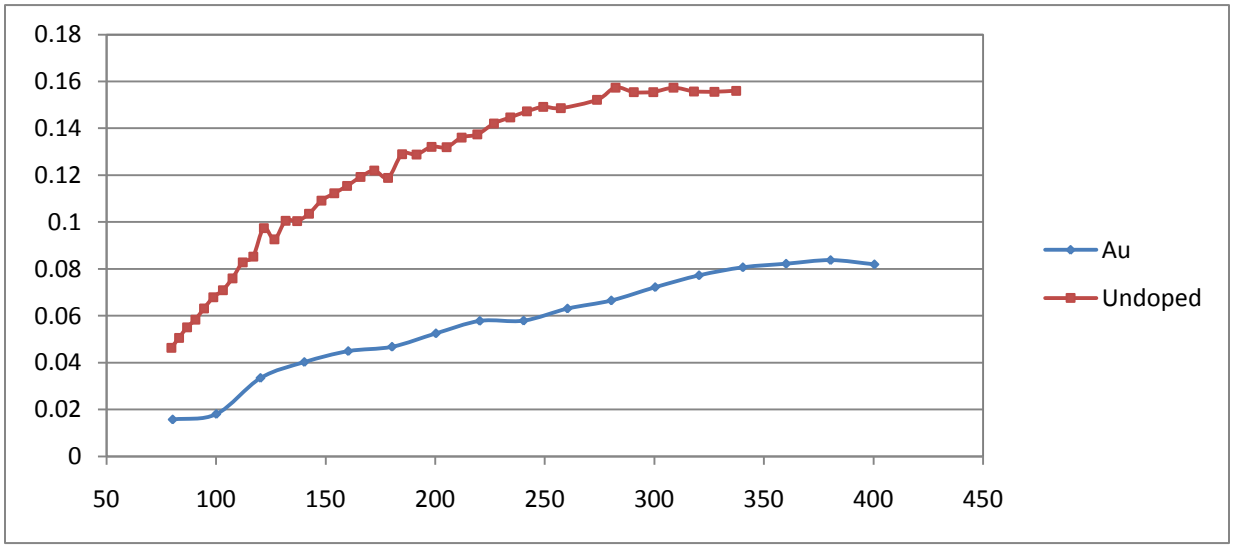

Figure 14: zT of Gold Doped Bismuth

4.3 Iridium

A composition of $Bi_{99.7}Ir_{0.3}$ was chosen based on its solubility in bismuth. The presence of iridium had little to no effect on thermal conductivity and electrical resistivity as seen in

Figure 15 and

Figure 16.
Figure 17 shows that the Seebeck decreased and as a result, the figure of merit was almost unaffected (Figure 18).

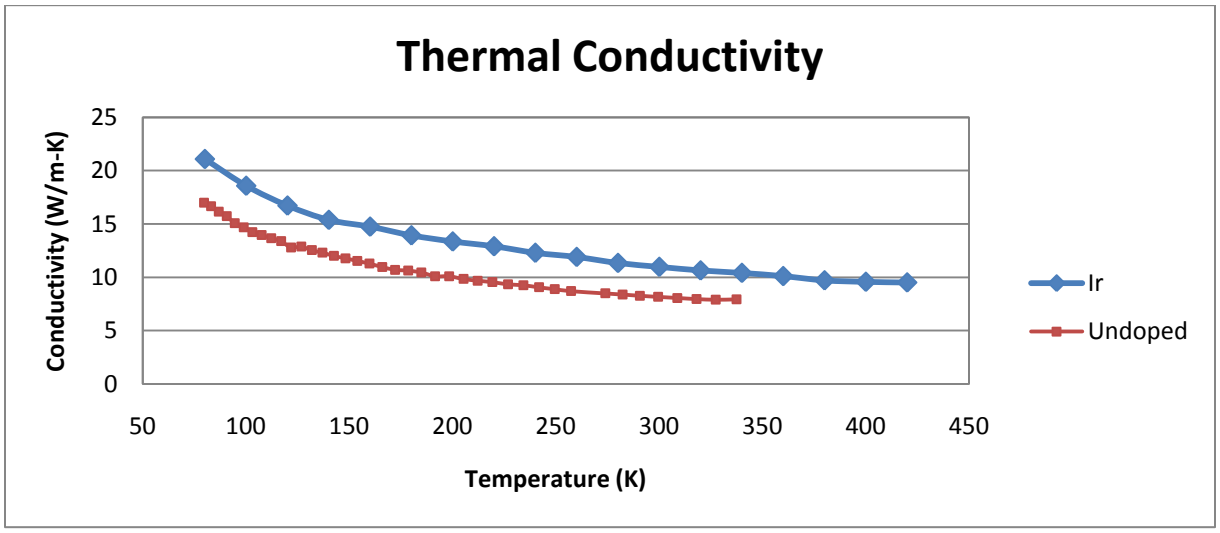

Figure 15:Thermal Conductivity of Iridium Doped Bismuth

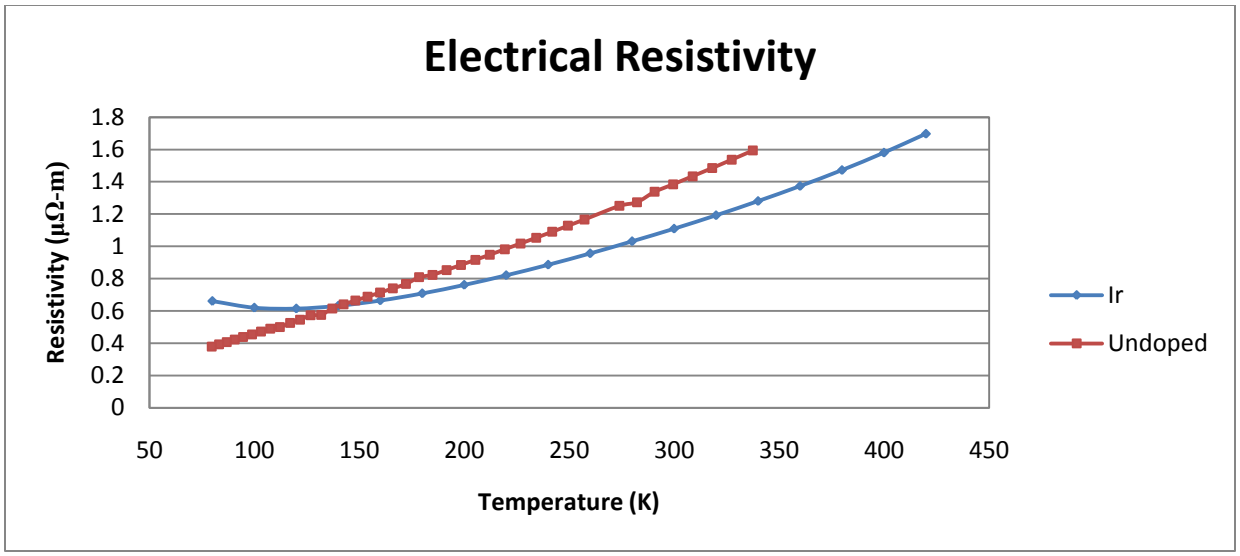

Figure 16: Electrical Resistivity of Iridium Doped Bismuth

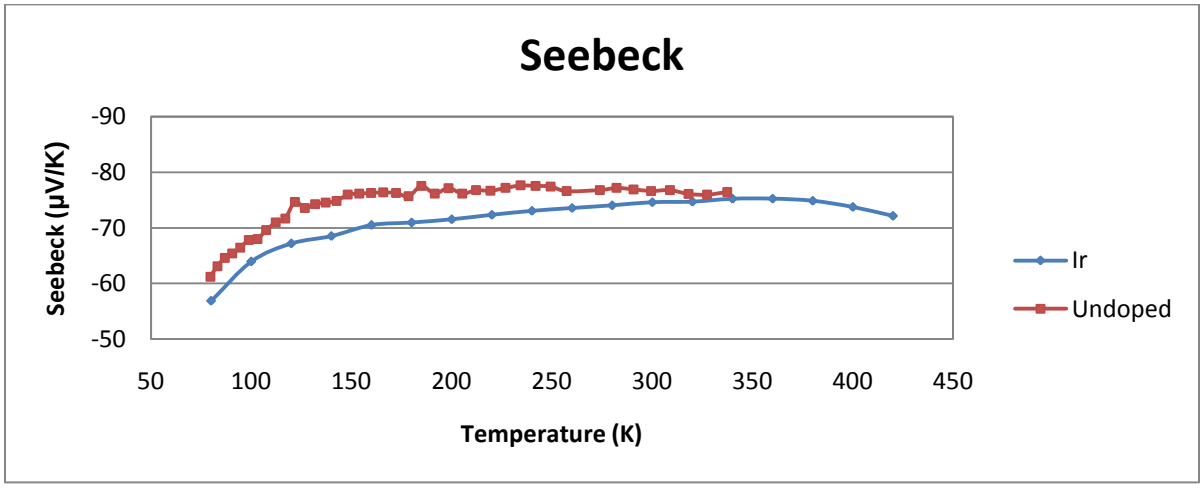

Figure 17: Seebeck of Iridium Doped Bismuth

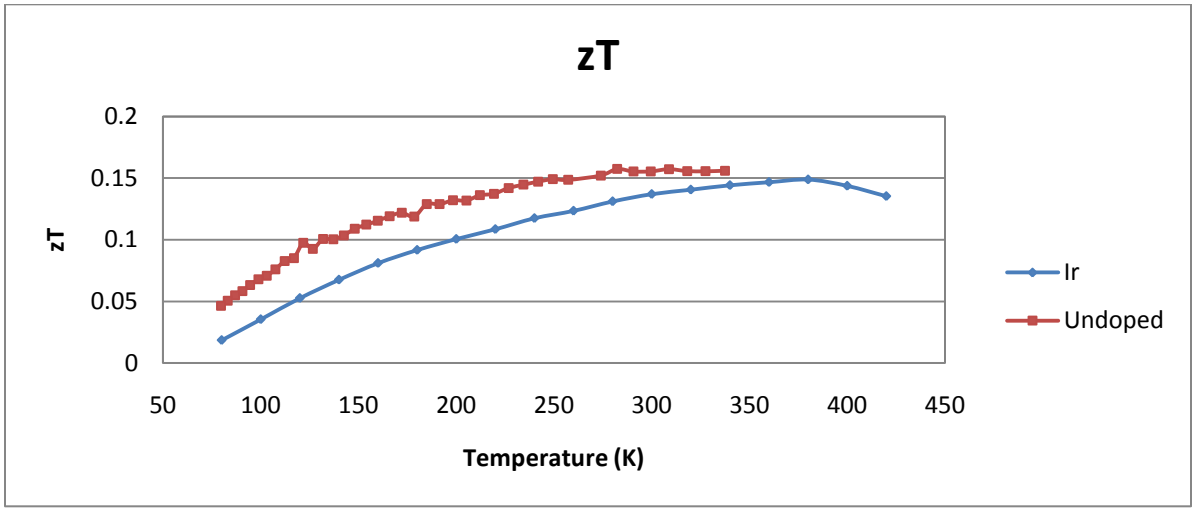

Figure 18: Figure of Merit of Iridium Doped Bismuth

4.4 Osmium

Osmium has a low solubility in bismuth, .0044 at % so a composition of $Bi_{99.8}Os_{0.2}$ was chosen for testing. The ppms was used to test this sample and found no change in thermal conductivity or electrical resistivity, as seen in

Figure *19* and

Figure *20*. Seebeck and therefore zT were lowered by the addition of Osmium as seen in Figure 21 and Figure 22

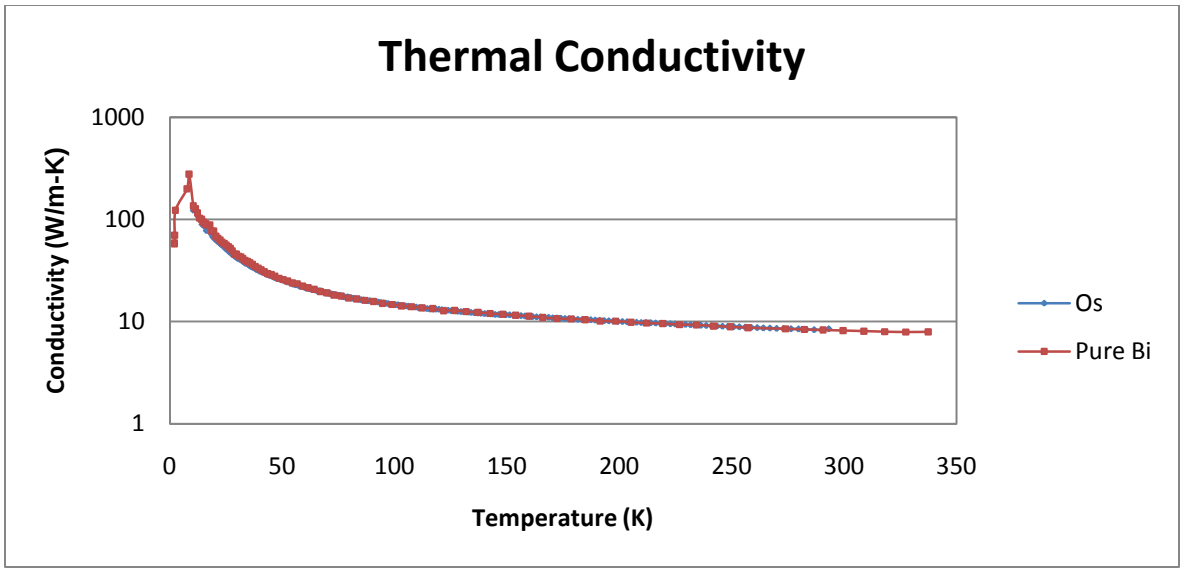

Figure 19: Thermal Conductivity of Osmium Doped Bismuth

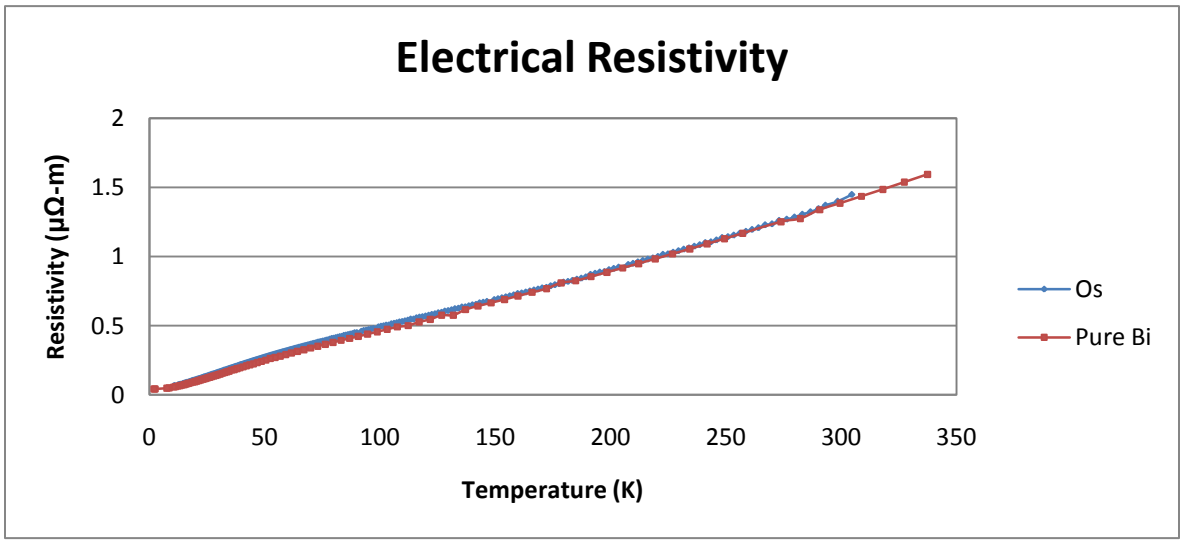

Figure 20: Electrical Resistivity of Osmium Doped Bismuth

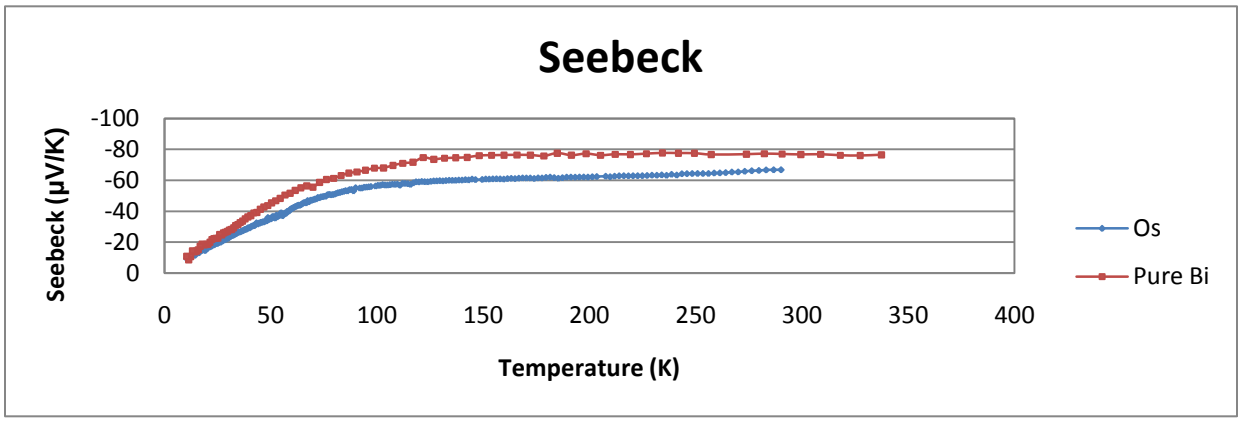

Figure 21: Seebeck of Osmium Doped Bismuth

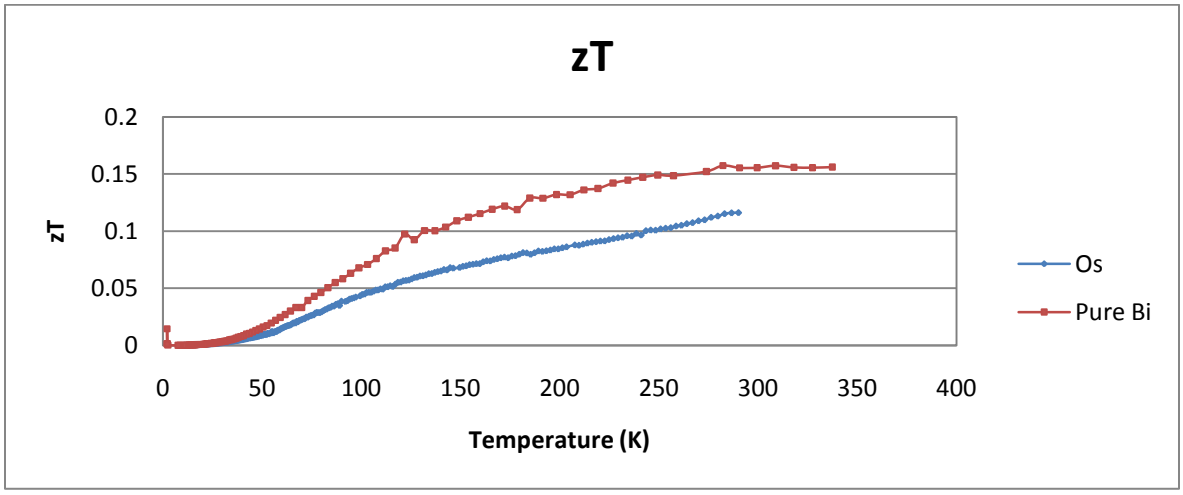

Figure 22: Figure of Merit of Osmium Doped Bismuth

4.5 Boron

A composition of 0.3% atomic percent Boron was used for testing. Boron had very little overall effect on the bismuth.

Figure 23 shows the thermal conductivity of the sample and shows a slight decrease from pure bismuth. The electrical resistivity was very similar to pure bismuth as seen in

Figure 24. Figure 25 and Figure 26 show Seebeck and zT respectively. Seebeck is slightly increased, but zT is decreased because of the increased thermal conductivity.

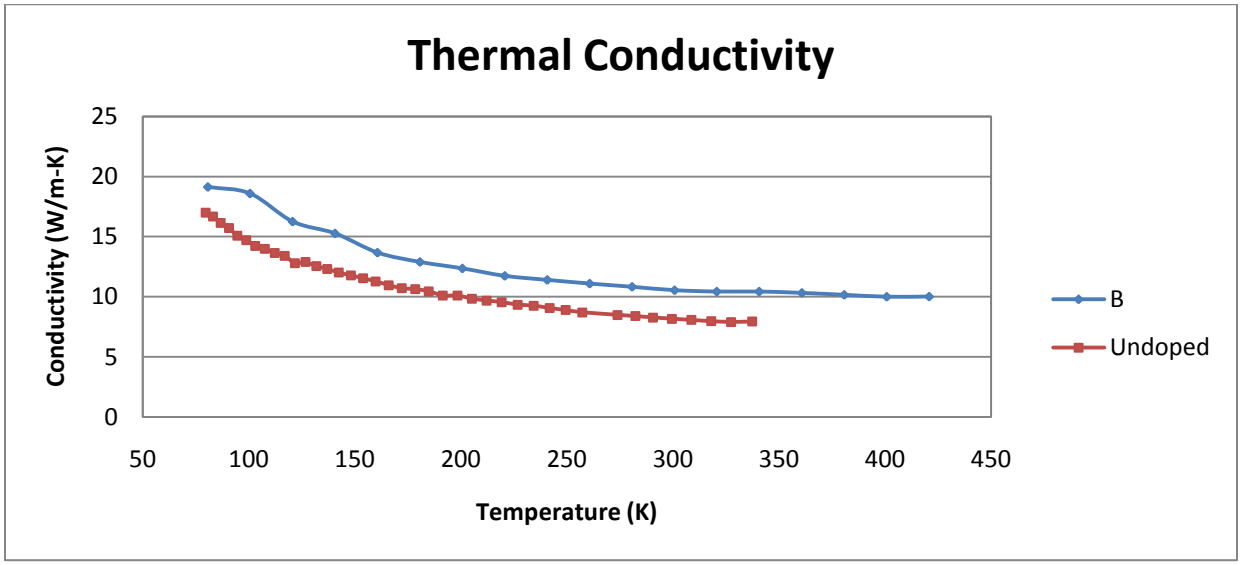

Figure 23: Thermal Conductivity of Boron Doped Bismuth

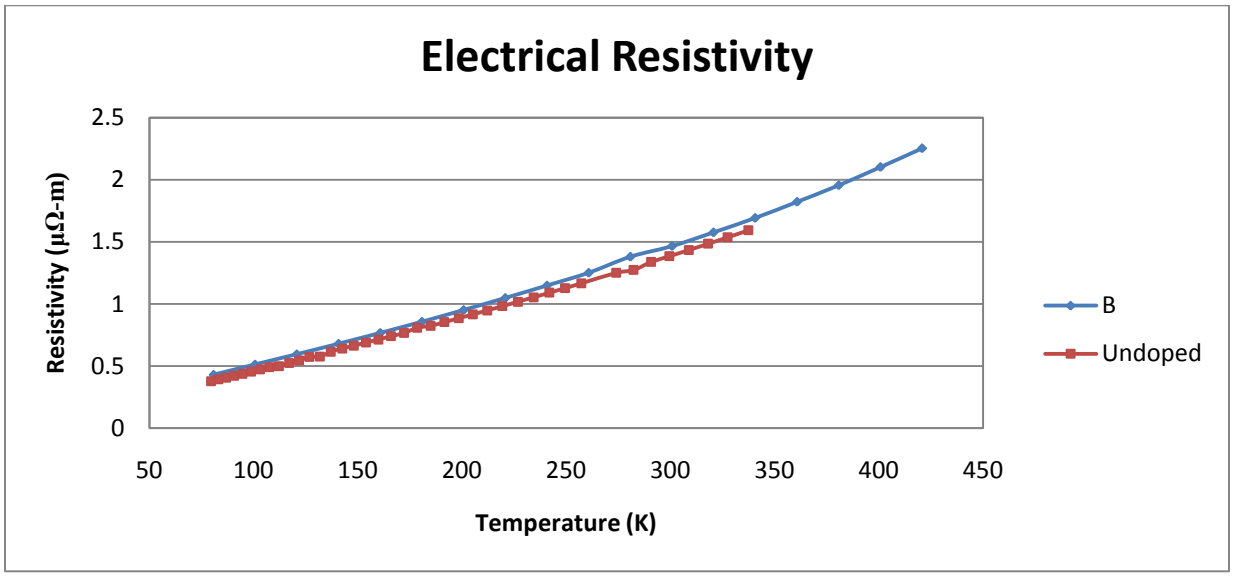

Figure 24: Electrical Resistivity of Boron Doped Bismuth

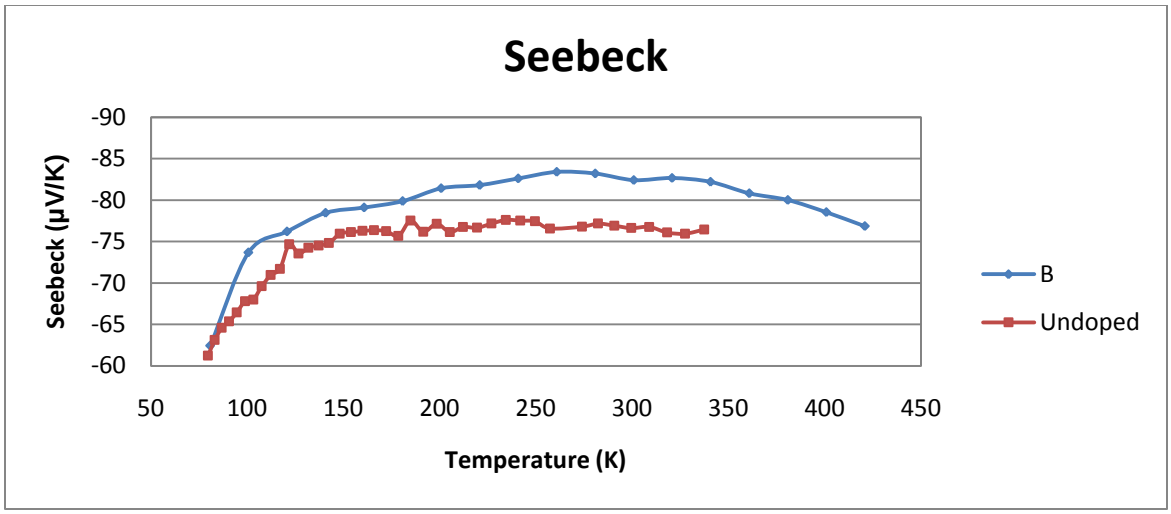

Figure 25: Seebeck of Boron Doped Bismuth

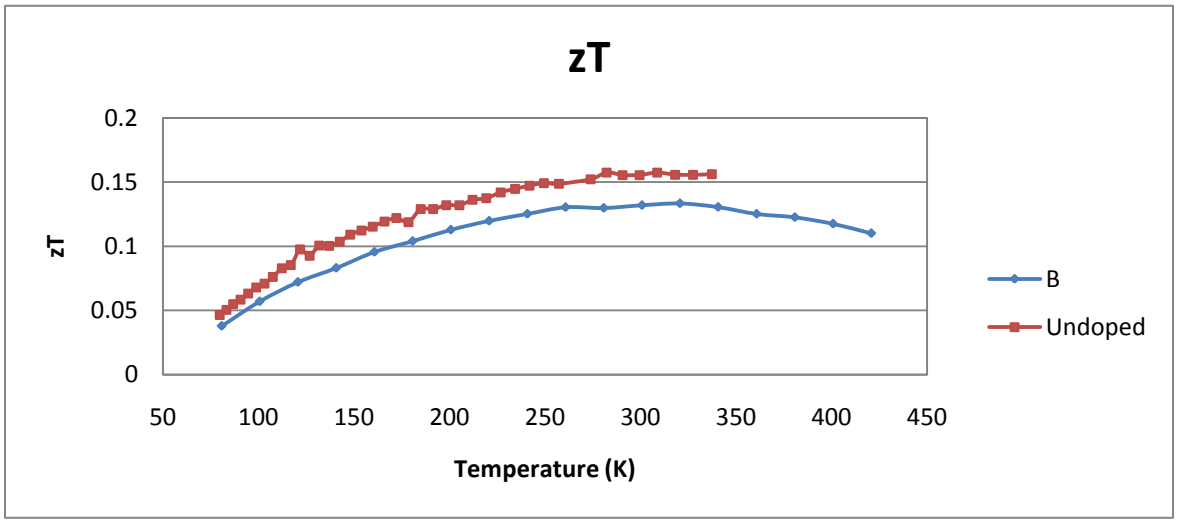

Figure 26: Figure of Merit of Boron Doped Bismuth

4.6 Aluminum

Aluminum has a relatively high solubility in bismuth compared to the other dopants at 1at%, so that is the composition chosen for testing. Aluminum had very little effect on the properties of bismuth besides electrical resistivity.

Figure 27 shows the comparison of thermal conductivities and very little difference can be seen. Electrical resistivity deviates from pure bismuth particularly at low temperatures as seen in

Figure 28.

Figure 29 shows Seebeck, which looks extremely similar to undoped bismuth. Figure 30 shows zT, which is reduced at low temperatures because of the increased electrical resistivity.

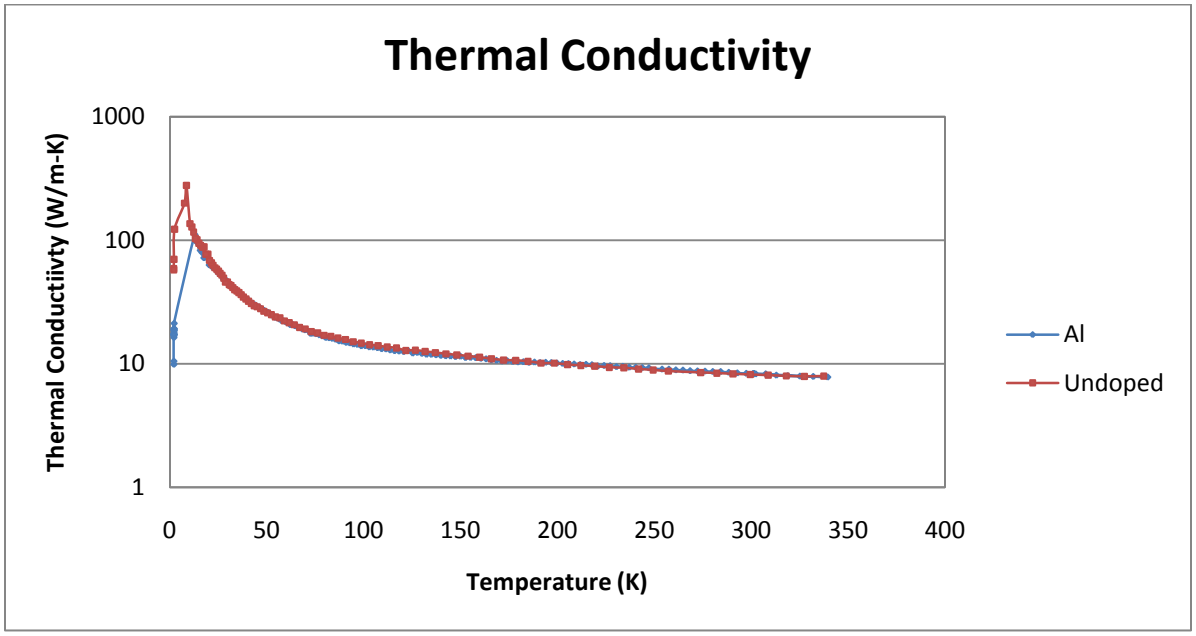

Figure 27: Thermal Conductivity of Aluminum Doped Bismuth

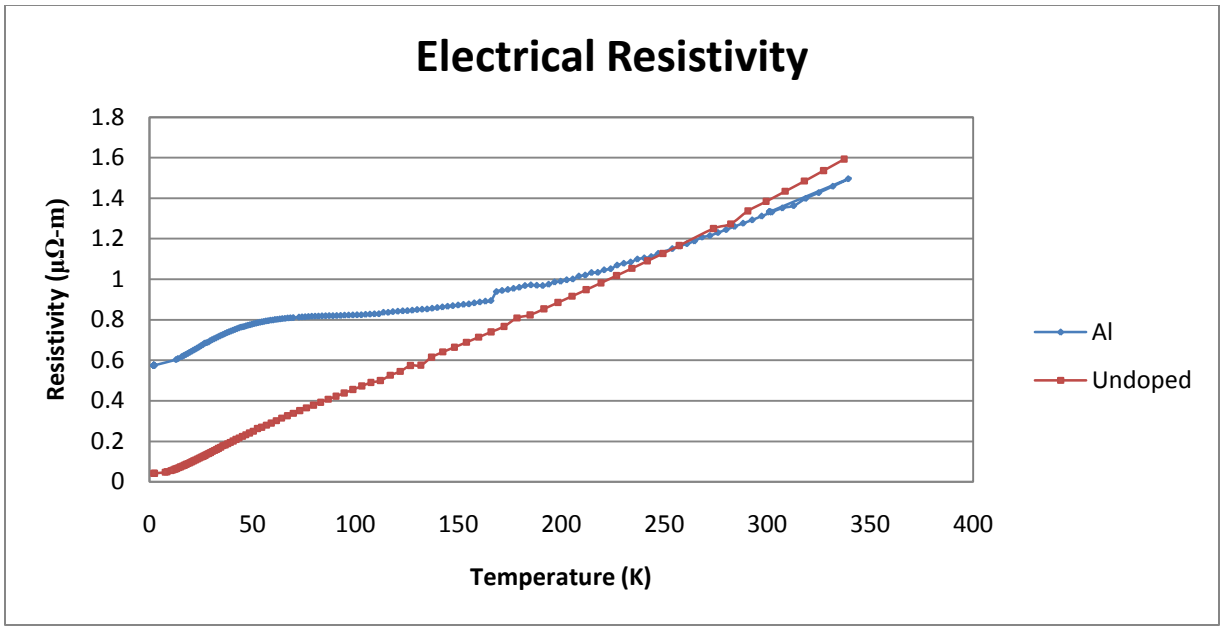

Figure 28: Electrical Resistivity of Aluminum Doped Bismuth

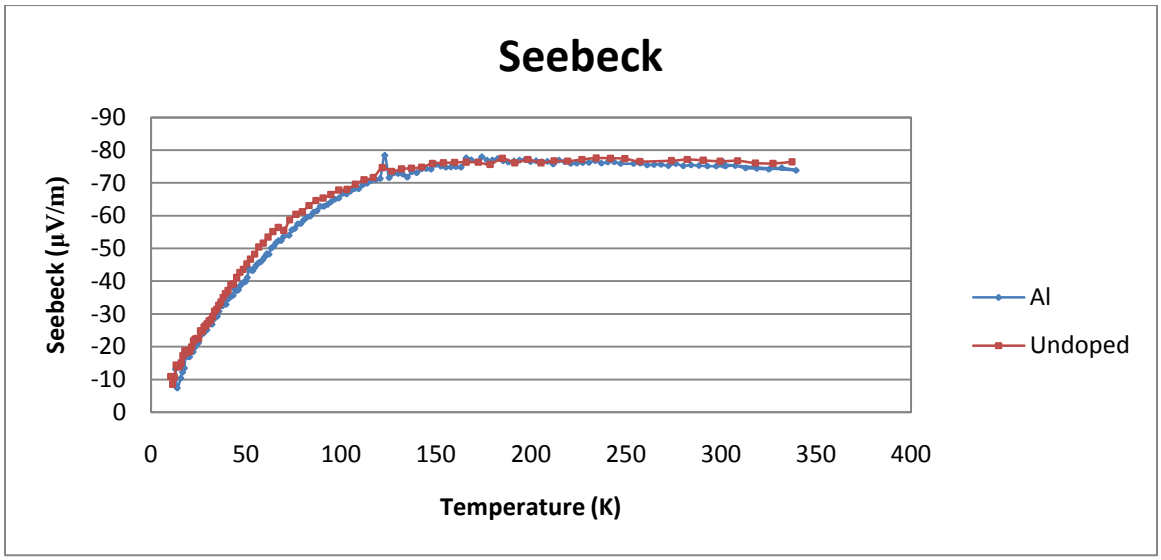

Figure 29: Seebeck of Aluminum Doped Bismuth

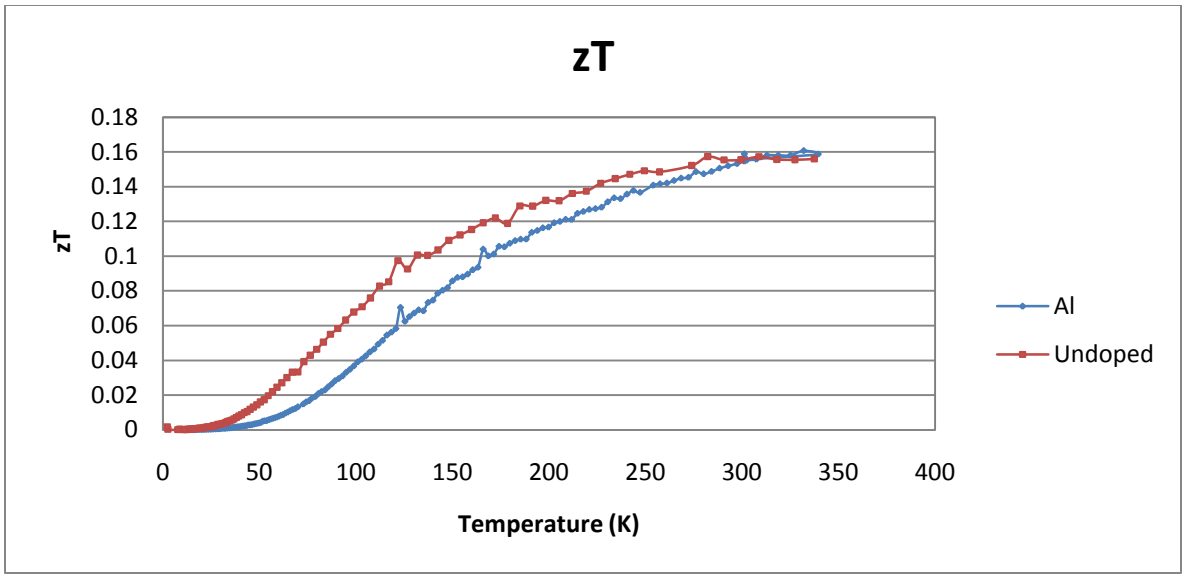

Figure 30: Figure of Merit of Aluminum Doped Bismuth

4.7 Gallium

$Bi_{99.5}Ga_{0.5}$ was also tested based on gallium's solubility in bismuth. Figure 31 show the thermal conductivity, which is virtually identical to that of pure bismuth. Gallium has an impact on electrical resistivity at low temperatures. This pattern is similar to that of the aluminum doped sample, but is has a higher magnitude at very low temperatures than aluminum, and can be seen in Figure 32. Seebeck is reduced in Figure 33. Figure 34 shows the zT which is reduced because of both the Seebeck and electrical resistivity.

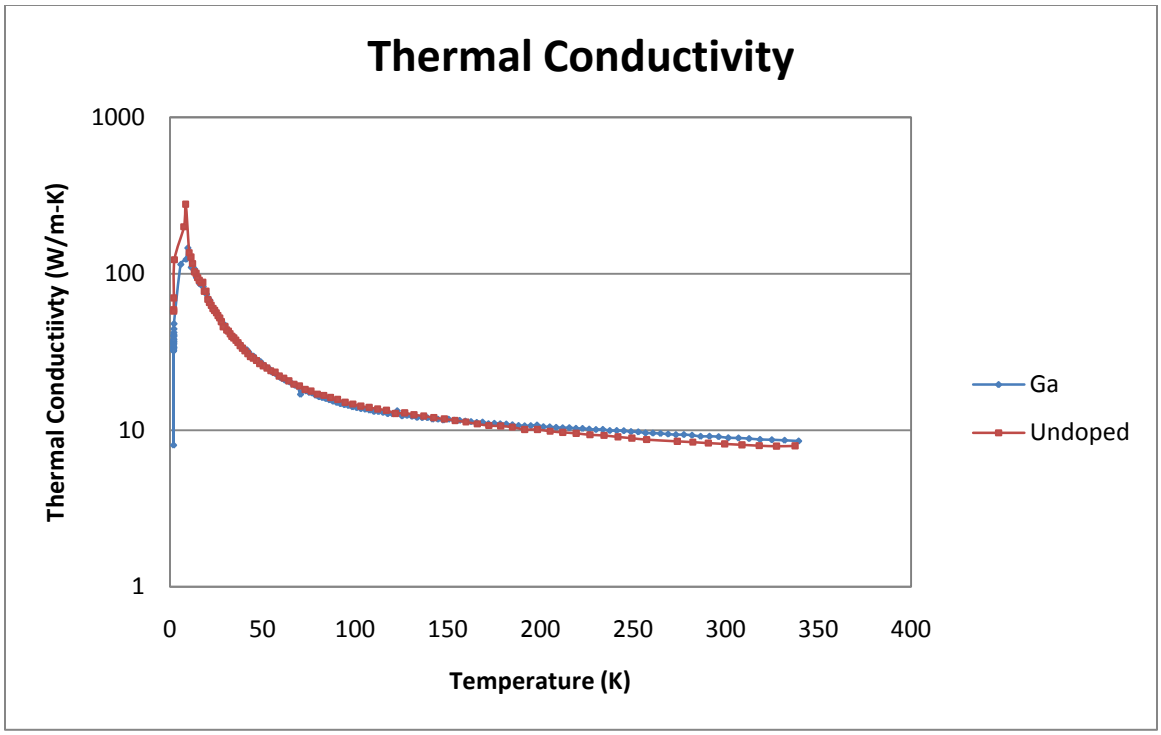

Figure 31: Thermal Conductivity of Gallium Doped Bismuth

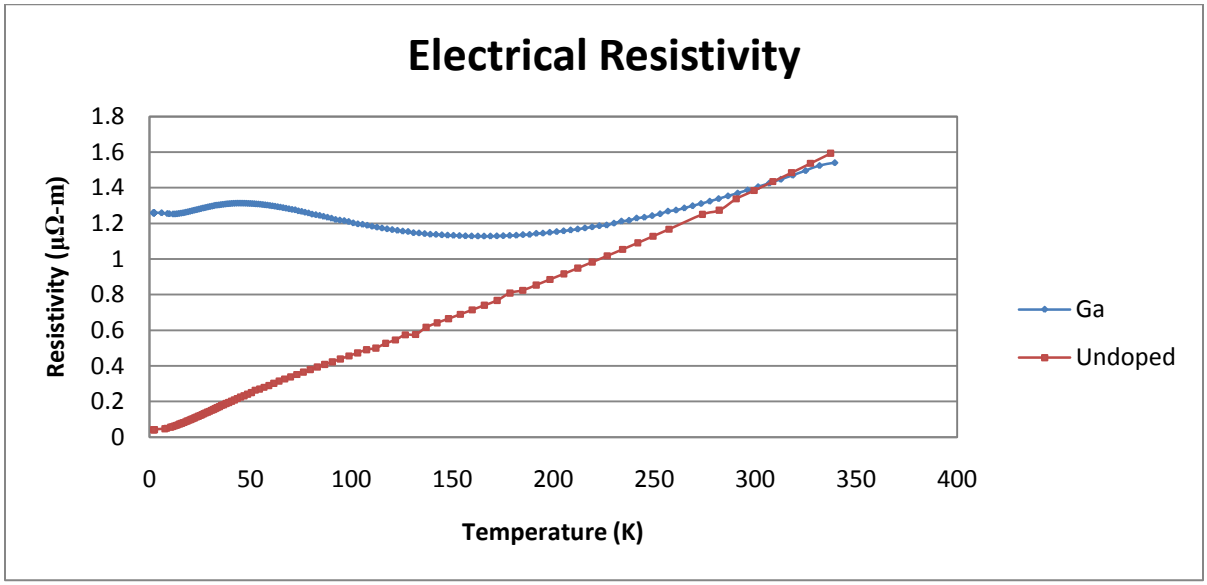

Figure 32: Electrical Resistivity of Gallium Doped Bismuth

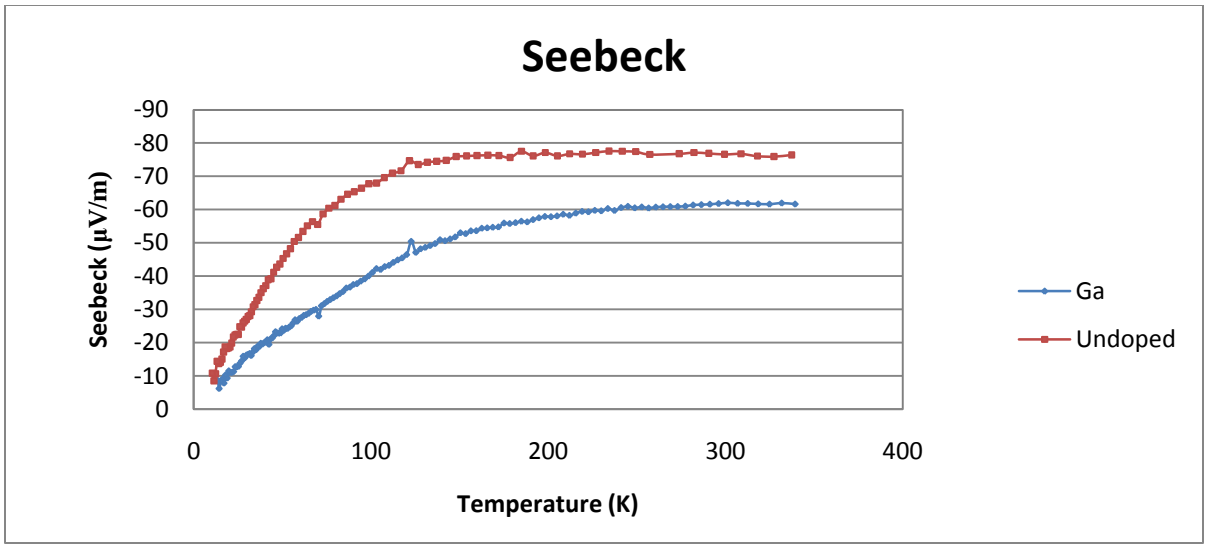

Figure 33: Seebeck of Gallium Doped Bismuth

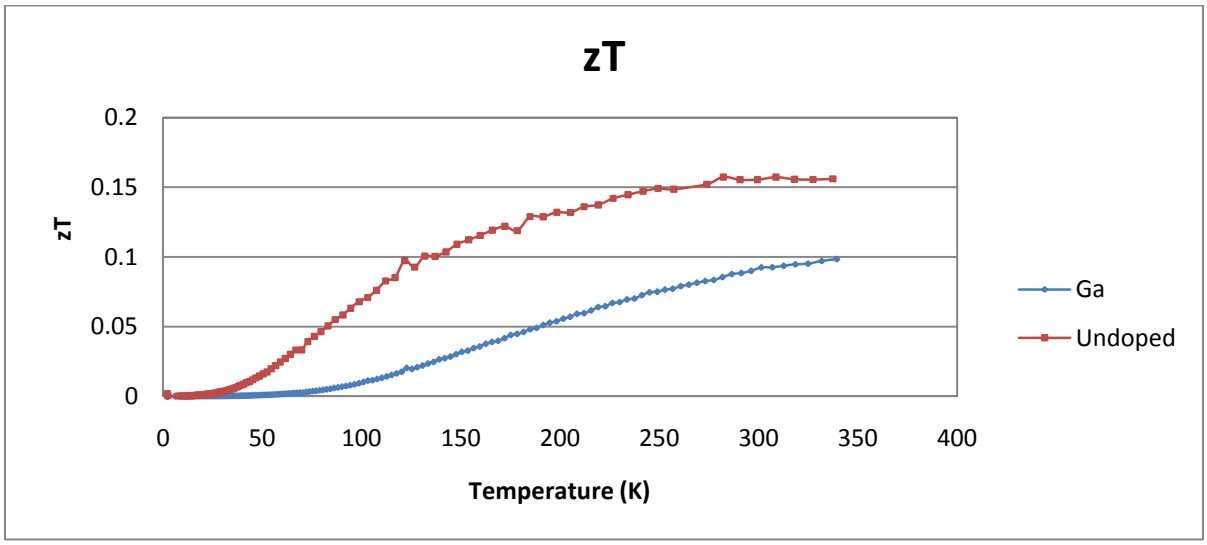

Figure 34: Figure of Merit of Gallium Doped Bismuth

4.8 Indium

Indium was by far the most interesting data collected. Indium has a higher solubility in bismuth than most elements, 0.5%. A sample was synthesized with a

composition of $Bi_{99.5}In_{0.5}$. The sample was later tested for its composition and found to be $Bi_{99.7}In_{0.3}$. Thermal conductivity was unaffected by the indium (Figure 35). Figure 36 show electrical resistivity of the sample. Electrical resistivity at room temperature was the same as pure bismuth, however at low temperatures, the resistivity increases before dropping off at very low temperatures. This indicates that indium acts as a p-typed donor in bismuth. Another indication that indium is a p-type donor in bismuth can be seen in Figure 37 showing Seebeck. At about 13K, Seebeck becomes positive before returning to zero near 0K. The magnitude of Seebeck is decreased compared to pure bismuth at temperatures below 95K, however, the magnitude of Seebeck is improved at temperatures above 95K, about a 20% improvement around 200K. The figure of merit is also improved as seen in Figure 38. Like the Seebeck coefficient, zT is decreased at low temperatures, but increased at temperatures above 175K. At room temperature, this represents a 44% increase in zT.

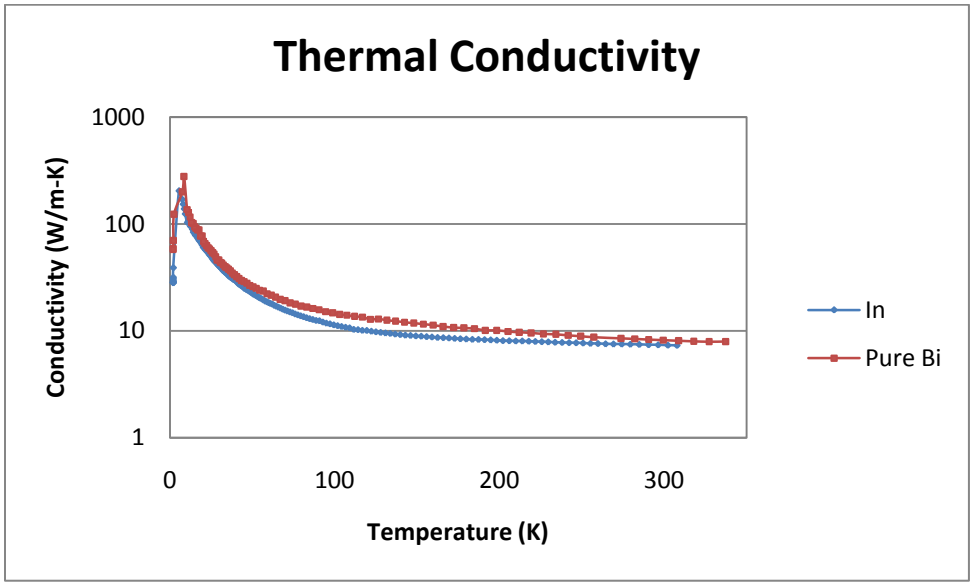

Figure 35: Thermal Conductivity of Indium Doped Bismuth

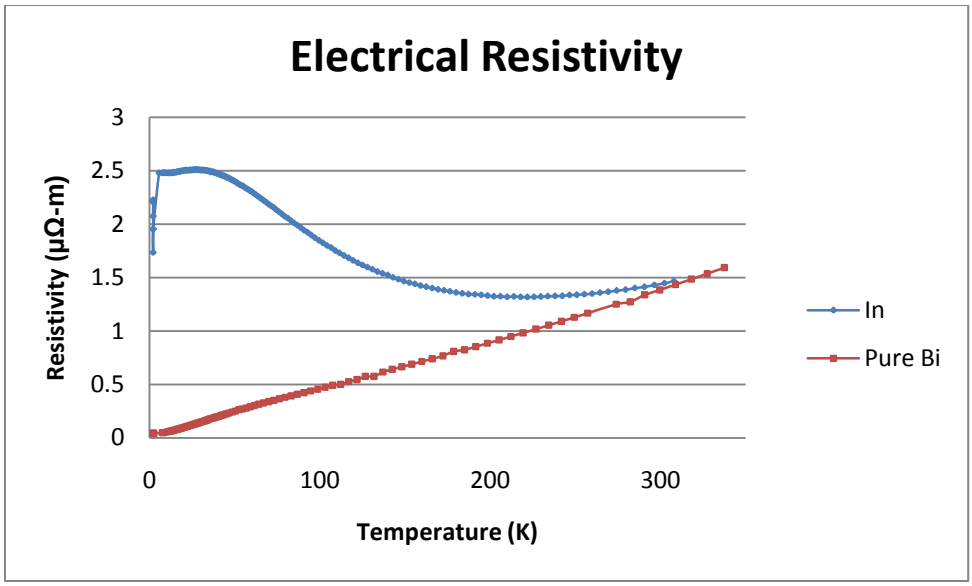

Figure 36: Electrical Resistivity of Indium Doped Bismuth

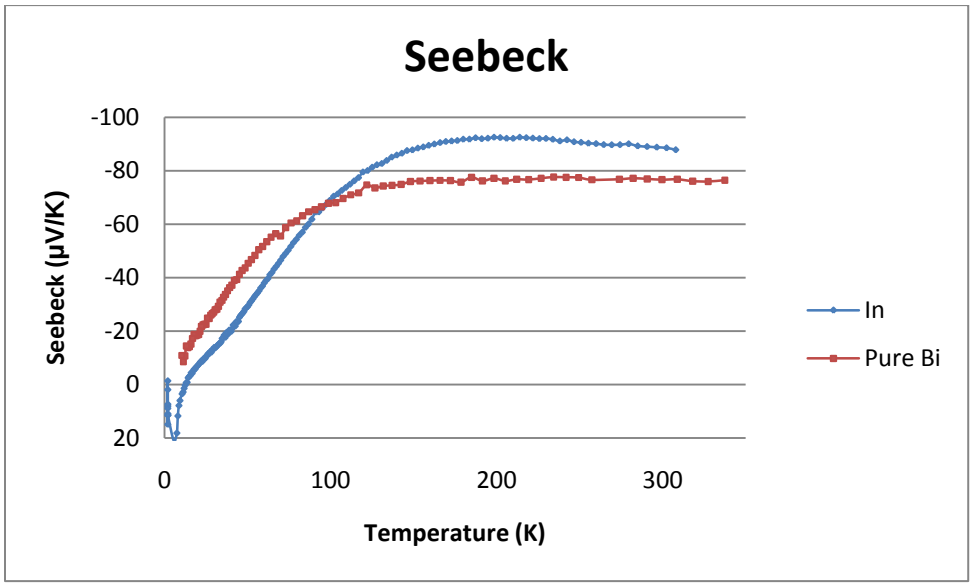

Figure 37: Seebeck of Indium Doped Bismuth

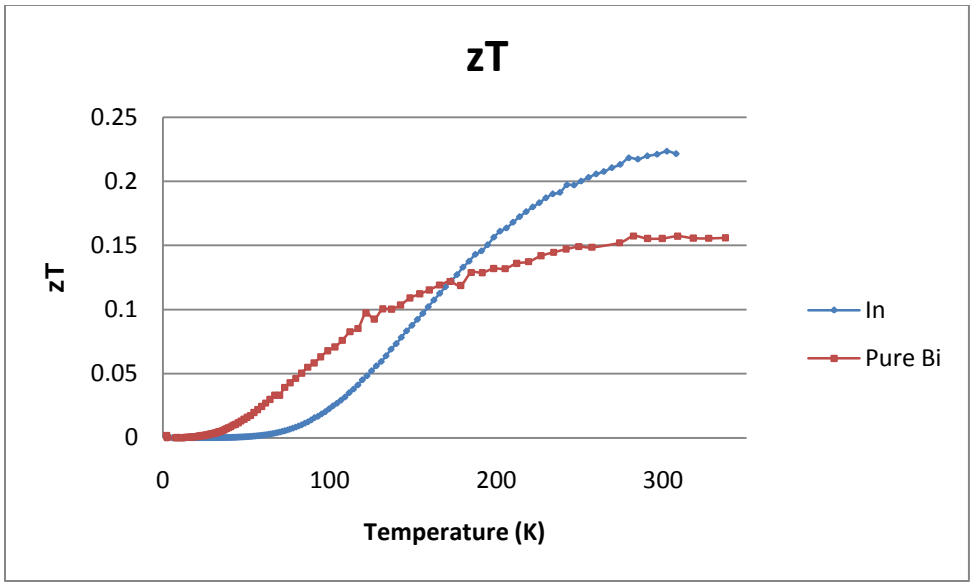

Figure 38: Figure of Merit of Indium Doped Bismuth

4.9 Conclusion

Of all the samples tested, Indium had the best results. It was able to increase the Seebeck and zT of bismuth significantly at temperatures above 200K, while not effecting electrical resistivity or thermal conductivity. Indium acts as a p-type donor in bismuth, which makes the resistivity high at low temperatures and a positive Seebeck at ever low temperatures. Based on these findings, further study of indium's effects on BiSb alloys has begun.

CHAPTER 5
NANO-PARTICLE BISMUTH ANTIMONY

5.1 Introduction

Originally, this research was focused on a new mixture of nano-particle bismuth antimony as well as the effects of adding alumina (Al_2O_3) for applications at or around room temperature. Currently the highest zT bismuth-antimony is $Bi_{88}Sb_{12}$, but some research suggested that $Bi_{96.5}Sb_{3.5}$ warranted investigation(Lenoir, Selme and Demouge). Two samples were made, one of pure bismuth-antimony and one at 5% alumina. Theoretically, nano-particles would allow electrons to pass while stopping phonons, decreasing thermal conductivity while not affecting electrical resistivity(Popescu, Woods and Martin). The inclusion of alumina was done based on the idea that alumina would filter holes to reduce the compensation between electrons and holes.

5.2 Experimental Procedure

The procedure for this experiment was very similar to the experimental procedure for the main part of the research. The major difference lies in the nano-particles. First, because of the nano-particles, the synthesis process was always done in the glove box. Nano-particles of bismuth and antimony oxidize very quickly because of their extremely high surface area to volume ratio and alumina tends to absorb water from the air. The samples were weight out to the same accuracy previously noted. In this case, they were

first placed in a steel grinding jar with several small stainless steel balls. This jar was sealed in the glove box while still in the glove box, then removed and placed in a ball mill for an hour. The ball mill would shake the sample and the stainless steel balls would crush the sample materials, creating the nano-particles. After the powder was created, the grinding jar was placed back in the glove box. The powder was measured into single gram samples, and placed in a graphite die. A 2-ton press was used to compress the sample. These samples were stacked in a quartz ampoule. As described previously, the gasses were evacuated and the sample sealed. Then, the sample would be annealed for about a week at 250°C, thus not melting the sample. The samples were then tested in the same fashion as the polycrystalline samples.

5.3 Results

Two samples of the $Bi_{96.5}Sb_{3.5}$ samples were successfully made and tested. One reference sample with no alumina and one sample with 5% alumina. Using the same process, samples of $Bi_{88}Sb_{12}$ doped with alumina were prepared by Hyungyu Jin. The $Bi_{96.5}Sb_{3.5}$ increased the thermal conductivity, compared to the $Bi_{88}Sb_{12}$ sample (Figure 39), which we expect from a decrease in alloy scattering. In both cases, the addition of alumina decreased the thermal conductivity. At 300K or above, all the samples except the $Bi_{88}Sb_{12}$ with 5% alumina sample had very similar electrical resistivity, seen in Figure 40. At low temperatures, the $Bi_{96.5}Sb_{3.5}$ had the lowest resistivity and with both formulas, the addition of 5% alumina increased resistivity. Figure 41 shows the Seebeck of the samples. Both the $Bi_{88}Sb_{12}$ samples had significantly higher Seebeck, particularly at low

temperatures. Again, the addition of alumina lowered the Seebeck with both formulas. The figure of merit for the samples is shown in

Figure 42 where the $Bi_{88}Sb_{12}$ sample showed the best results.

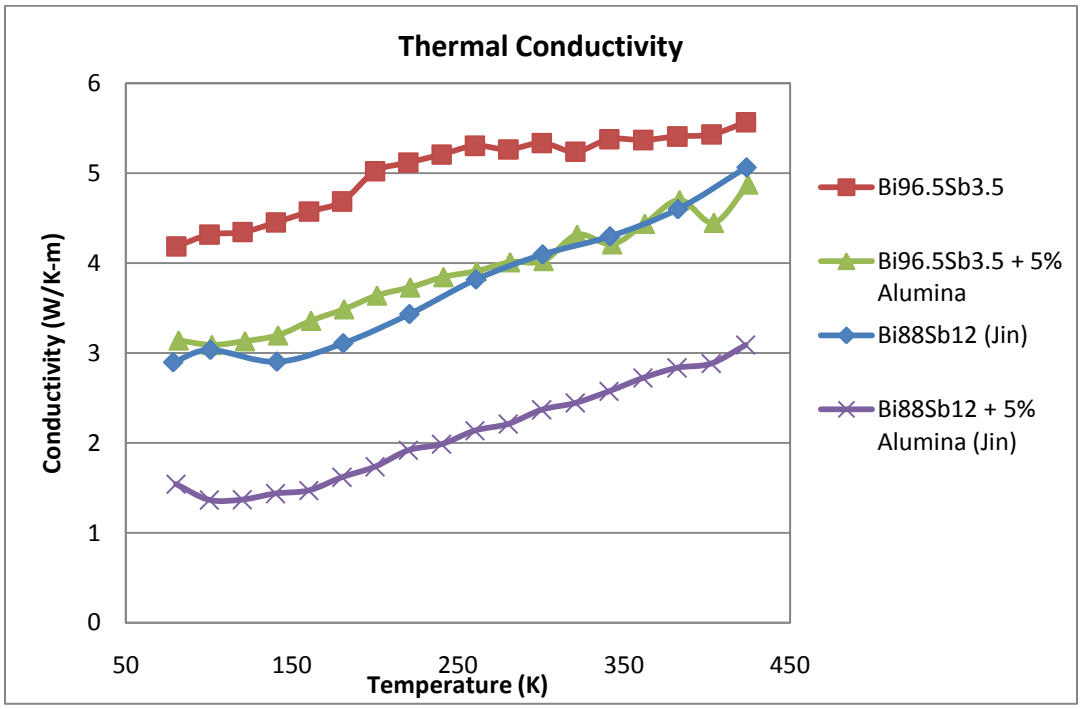

Figure 39: Thermal Conductivity of Nano-Particle Bismuth Antimony

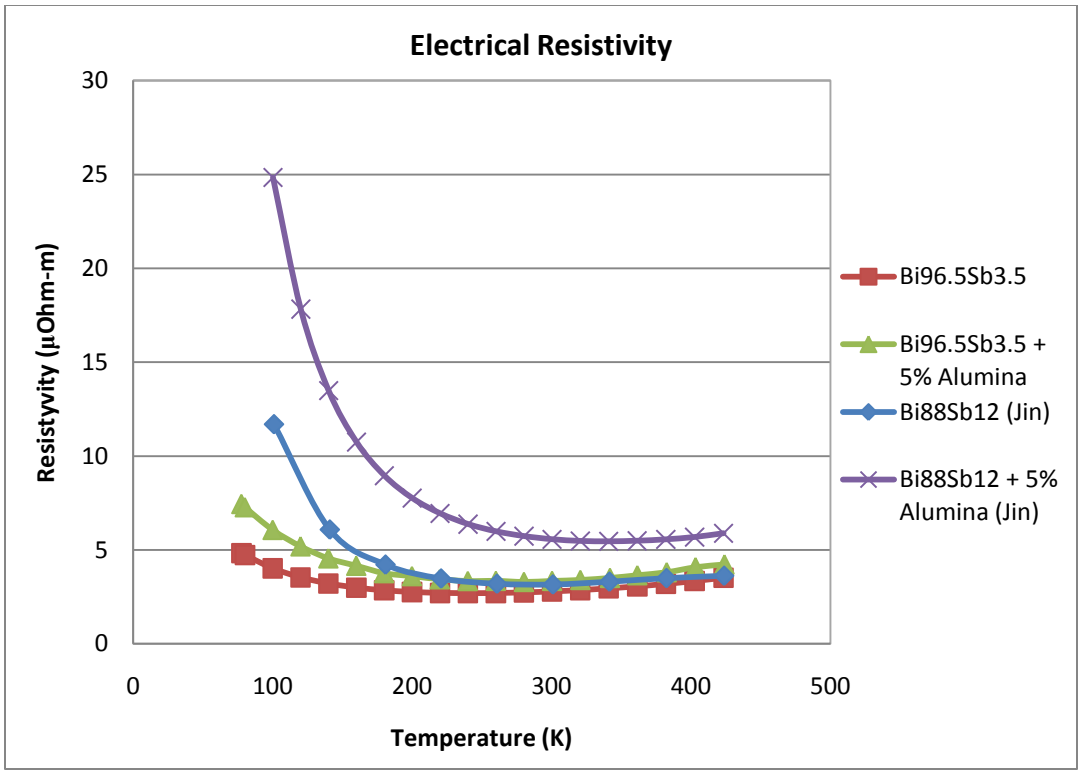

Figure 40: Electrical Resistivity of Nano-Particle Bismuth Antimony

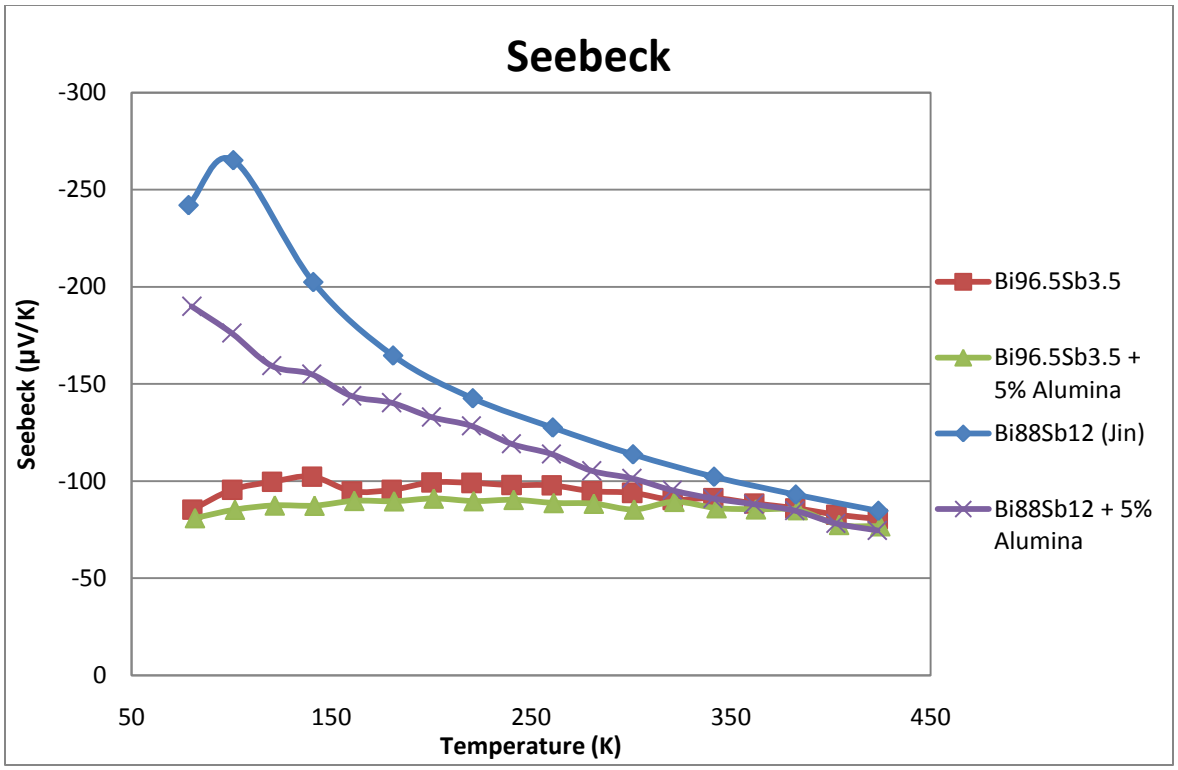

Figure 41: Seebeck Coefficient of Nano-Particle Bismuth Antimony

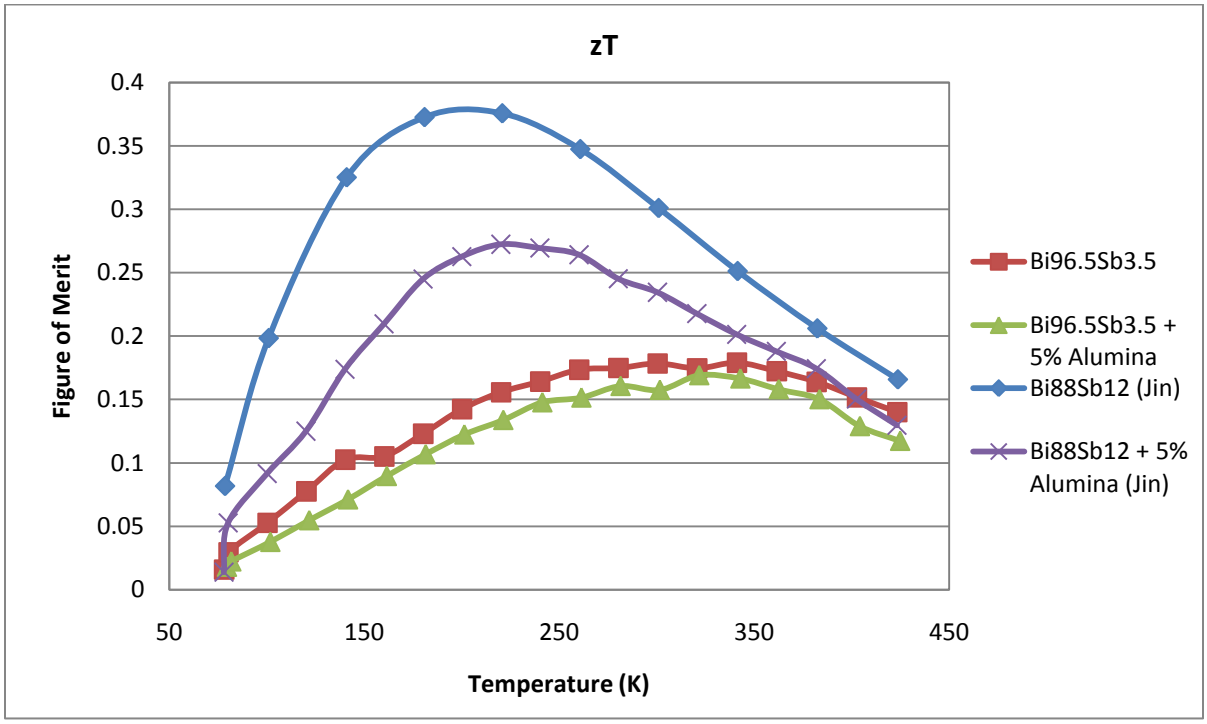

Figure 42: Figure of Merit of Nano-Particle Bismuth Antimony

5.4 Conclusion

The $Bi_{96.5}Sb_{3.5}$ showed slight improvement in the electrical resistivity, however, it worsened thermal conductivity and Seebeck resulting in a large loss in zT. The addition of 5 % alumina improved thermal conductivity, but also increased electrical resistivity and decreased Seebeck, leading to a reduction in zT. Overall, the $Bi_{96.5}Sb_{3.5}$ did not result in a material comparable to the current bismuth-antimony leader $Bi_{88}Sb_{12}$ and does not warrant further study. The addition of 5% alumina acted as predicted in decreasing thermal conductivity, however, it negatively impacted the other properties. While 5% alumina was not successful, other concentrations of alumina may have better results.

CHAPTER 7
FUTURE WORK AND CONCLUSION

This project aimed to develop the foundation for improving the efficiency of bismuth-antimony alloys by studying the effects of dopants. Of the polycrystalline bismuth tests, indium was the only sample to improve the material's zT. Indium was able to improve both Seebeck and zT without impacting thermal conductivity or electrical resistivity. Further research into indium doped bismuth-antimony alloys will show weather these results will have an impact on practical materials.

The new formula of $Bi_{96.5}Sb_{3.5}$ could not compare to $Bi_{88}Sb_{12}$ in terms of overall efficiency. The addition of 5% alumina also did not improve upon the efficiencies of Bismuth-Antimony alloys alone. Other amounts of alumina may yield different results.

WORKS CITED

Dawson, Bryan. Nobel Prize Winners and Famous Hungarians. 5 November 2010 <http://www.americanhungarianfederation.org/FamousHungarians//sciencemathandtech2.htm>.

Heremans, Joseph, et al. "Enhancement of Thermoelectric Efficiency in PbTe by Distortion of the Electronic Density of States." Science (2008): 554.

Jaworski, Christopher. "New High-zT Thermoelectric Materials for Solar and Waste Heat Applications." Poster. 2008.

Lenoir, B, et al. "Electron and Hole Transport in undoped Bi0.96Sb0.04 alloys." The American Physical Society 1 May 1998: 242-250.

Popescu, A., et al. A Model of Transport Properties of Thermoelectric Nanocomposite Materials. Tampa, Florida: Department of Physics, University of South Florida, n.d.

Stein, Charles. "Relevence of Solid State Cooling for Air Force Needs." 1 September 2010.